
Top quark working group report

1 Draft date: August 2, 2013

2 **Conveners: K. Agashe, R. Erbacher, C. E. Gerber, K. Melnikov,**
3 **R. Schwienhorst.**

4 **Contacts by topic:** A. Mitov, M. Vos, S. Wimpenny (top mass); J. Adelman, M. Baumgart,
5 A. Garcia-Bellido. A. Loginov (top couplings); A. Jung, M. Schulze, J. Shelton (kinematics); N. Craig,
6 M. Velasco (rare decays); T. Golling, J. Hubisz, A. Ivanov, M. Perelstein (new particles); S. Chekanov,
7 J. Dolen, J. Pilot, R. Pöschl, B. Tweedie (detector/algorithm).

8 **Contributors:** S. Alioli, B. Alvarez-Gonzalez, D. Amidei, T. Andeen, A. Arce, B. Auerbach, A. Avetisyan,
9 M. Backovic, Y. Bai, M. Begel, S. Berge, C. Bernard, C. Bernius, S. Bhattacharya, K. Black, A. Blondel,
10 K. Bloom, T. Bose, J. Boudreau, J. Brau, G. Brooijmans, E. Brost, R. Calkins, D. Chakraborty,
11 T. Childress, G. Choudalakis, V. Coco, J.S. Conway, C. Degrande, A. Delannoy, F. Deliot, L. Dell’Asta,
12 E. Drueke, B. Dutta, A. Effron, K. Ellis, J. Erdmann, J. Evans, C. Feng, E. Feng, A. Ferroglia, K. Finelli,
13 W. Flanagan, I. Fleck, A. Freitas, F. Garbersson, R. Gonzalez Suarez, M. Graesser, N. Graf, Z. Greenwood,
14 C. Group, A. Gurrola, G. Hammad, T. Han, Z. Han, U. Heintz, S. Hoeche, T. Horiguchi, A. Ismail,
15 P. Janot, W. Johns, J. Joshi, A. Juste, T. Kamon, C. Kao, Y. Kats, A. Katz, M. Kaur, R. Kehoe,
16 W. Keung, S. Khalil, A. Khanov, N. Kidonakis, C. Kilic, N. Kolev, A. Kotwal, J. Kraus, D. Krohn,
17 M. Kruse, S. Lee, E. Luiggi, S. Mantry, A. Melo, D. Miller, G. Moortgat-Pick, M. Narain, N. Odell,
18 Y. Oksuzian, M. Oreglia, A. Penin, Y. Peters, C. Pollard, S. Poss, J. Proudfoot, S. Rappoccio, S. Redford,
19 M. Reece, F. Rizatdinova, P. Roloff, R. Ruiz, M. Saleem, B. Schoenrock, C. Schwanenberger, T. Schwarz,
20 K. Seidel, E. Shabalina, P. Sheldon, F. Simon, K. Sinha, P. Skands, P. Skubik, G. Sterman, D. Stolarski,
21 J. Strube, J. Stupak, S. Su, M. Tesar, S. Thomas, E. Thompson, P. Tipton, E. Varnes, N. Vignaroli,
22 J. Virzi, M. Vogel, D. Walker, K. Wang, B. Webber, J.D. Wells, S. Westhoff, D. Whiteson, M. Williams,
23 S. Wu, U. Yang, H. Yokoya, H. Yoo, H. Zhang, N. Zhou, H. Zhu, J. Zupan.

24 1.1 Introduction

25 The top quark was discovered in 1995 [1, 2] and it is still the heaviest elementary particle known today.
26 Thanks to its large mass, and the related strength of its coupling to the Higgs boson, the top quark may
27 be a key player in understanding the details of electroweak symmetry breaking. Studies of the top quark
28 properties at the Tevatron and Run I of the LHC have given us a detailed understanding of many properties
29 of this particle, including its mass, production and decay mechanisms, electric charge and more. With
30 the exception of the large forward-backward asymmetry in $t\bar{t}$ production that has been observed at the
31 Tevatron, all results on top quark pairs and single top production obtained so far have been consistent with
32 the Standard Model.

33 In the short and mid-term future top quark studies will be mainly driven by the LHC experiments. Explora-
34 tion of top quarks will, however, be an integral part of particle physics studies at any future facility. Future
35 lepton colliders will have a rich top quark physics program which would add to our understanding of this
36 interesting quark. Detailed simulation studies have been carried out for linear electron-positron machines

(ILC and CLIC). First attempts have been made to extrapolate these to the case of a circular machine (TLEP). In this report we describe what can be achieved based on projection studies for the LHC and for future lepton colliders. The report is organized along six topics:

- Measurement of the top quark mass;
- Studies of kinematic distributions of top-like final states;
- Measurements of top quark couplings;
- Searches for rare decays of top quarks;
- Probing physics beyond the Standard Model with top quarks;
- Algorithms and detectors for top quark identification at future facilities.

Main conclusions for each topic are presented in Sect.1.8

1.2 The top quark mass

The top quark mass is a parameter whose precise value is essential for testing the overall consistency of the Standard Model or models of New Physics through precision electroweak fits. The exact value of the top quark mass is also crucial for understanding whether the Standard Model *without further extensions* can be continued to energies compared to the Planck scale, without running into problems with the stability of electroweak vacuum [3]. To put both of these statements into perspective, we note that the value of the top quark mass, as quoted by the Particle Data Group, is $m_t = 173.5 \pm 0.6 \pm 0.8$ GeV. The total uncertainty on m_t is therefore close to 1 GeV; this is the best relative precision available for *any* of the quark masses.

Nevertheless, we know that for precision electroweak fits, a 0.6 GeV uncertainty in the top quark mass corresponds to a 5 MeV uncertainty in the W -mass (see e.g. Refs. [4]). Since the W -mass is expected to be measured with this precision at future facilities, but significant improvements in δM_W beyond this are not likely, we conclude that the future of precision electroweak physics requires the measurement of the top quark mass to at least a precision of less than 0.6 GeV, and desirably to 0.3 GeV so that the top sector is not limiting in EW precision fits.

On the other hand, the vacuum stability issue depends strongly on the value of the top quark mass. Indeed, as shown in Ref. [3], changing m_t by 2.1 GeV around the central value $m_t = 173.1$ GeV, the RGE scale where the Higgs quartic coupling becomes negative changes by *six* orders of magnitude, from $\mu_{\text{neg}} \sim 10^8$ GeV to $\mu_{\text{neg}} \sim 10^{14}$ GeV! It is easy to estimate that if m_t is known with 0.3 – 0.5 GeV uncertainty, as required by the electroweak fit, the scale can be estimated much more precisely, $\mu_{\text{neg}} \sim (4.8 \pm 1.2) \times 10^{13}$ GeV. We conclude that the knowledge of the top quark mass with the 0.5 GeV uncertainty will have an important impact on our understanding of particle physics.

Furthermore, it has recently been suggested [5] that a much more precise measurement of the W mass can be performed at a circular e^+e^- collider such as TLEP, where $\delta M_W \leq 1.5$ MeV can probably be achieved. For the purpose of precision electroweak fits, such high precision can be only utilized if the top quark mass is measured with the matching precision of about 0.1 GeV. As we explain below this can be accomplished at an e^+e^- collider such as the ILC, CLIC or TLEP itself. Knowing m_t with such a precision will allow for a much more decisive tests of the vacuum stability problem in the Standard Model. The interest in testing this scenario may increase greatly if no new physics at the TeV scale is found in the Run II of the LHC.

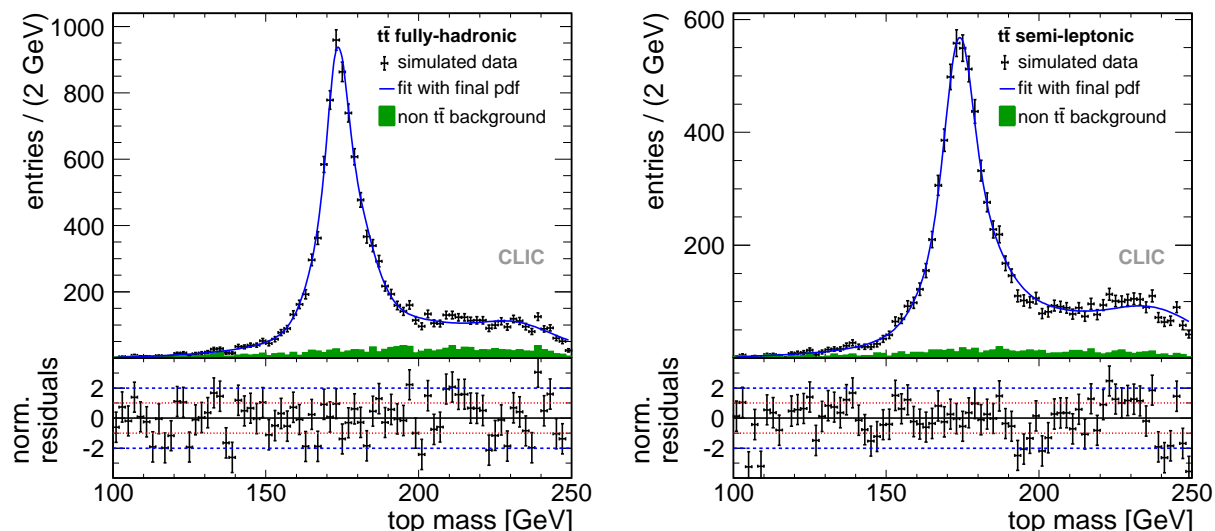


Figure 1-1. Distribution of reconstructed top mass for events classified as fully-hadronic (left) and semileptonic (right). The data points include signal and background for an integrated luminosity of 100 fb^{-1} . The pure background contribution contained in the global distribution is shown by the green solid histogram. The top mass is determined with an unbinned likelihood fit of this distribution, which is shown by the solid line.

1.2.1 Linear Colliders

A e^+e^- collider will allow us to study electroweak production of $t\bar{t}$ pairs with no concurring QCD background. Therefore, precise measurements of top quark properties become possible.

The top quark mass can be measured at the e^+e^- machine using two complementary methods. First, one can use the invariant mass of the reconstructed bW system from the top decay. The result of a full simulation study at a 500 GeV ILC [6] is shown in Fig. 1-1. The figure demonstrates also the small residual background expected for top quark studies at any e^+e^- machines. In the second method the top mass is determined in a threshold scan, an option unique to an e^+e^- machine. In the threshold scan the top mass can be measured to an experimental precision of better than 40 MeV where studies have shown that the statistical error is dominant. Expressing the measurement in the theoretically well defined $\overline{\text{MS}}$ mass will inflate the uncertainty to ~ 100 MeV, as shown in detailed simulations [7, 6, 8] and advanced theoretical computations (see e.g. Ref. [9] and references therein).

We note that with respect to the top quark mass determination, all lepton colliders that were suggested so far perform similarly¹ and that an additional attraction of measuring m_t at a lepton collider is a clean theoretical interpretation of the result of the measurement. As we explain below, the situation is more confusing at a hadron collider although new methods for m_t measurements developed at the LHC help to mitigate this difference.

In the threshold scan the top mass can be measured to a precision of better than 40 MeV where systematic studies have shown that the statistical error is dominant. However, using the $\overline{\text{MS}}$ mass will inflate the uncertainty to ~ 100 MeV.

¹We note that some improvements in the m_t determination can be expected at the muon collider and at TLEP thanks to reduced beamstrahlung, although this still has to be demonstrated by detailed simulations.

1.2.2 Top quark mass at the LHC

As previously noted, a precision of 0.5 GeV or better in the top quark mass is motivated by the future of precision electroweak fits. It is an interesting question whether m_t measurements with such a precision can be accomplished at the LHC. To answer it, we will first make some general remarks about measurements of m_t .

Existing measurements of the top quark mass rely on complex techniques required by the difficult hadron collider environment. The highest accuracy is currently achieved using the so-called matrix-element method (for a recent review, see [10]). We will explain a generic measurement of the top quark mass by considering the following example. Any measurement of the top quark mass is based on fitting a particular piece of data to a theory prediction where m_t enters as a free parameter. Hence, we write

$$D = T(m_t, \alpha_s, \Lambda_{\text{QCD}}) = T^{(0)}(m_t) + \frac{\alpha_s}{\pi} T^{(1)}(m_t) + \mathcal{O}(\Lambda_{\text{QCD}}/m_t, \alpha_s^2), \quad (1.1)$$

where D on the left hand side is a particular kinematic distribution measured in experiment and T on the right-hand side is a theoretical prediction, expanded in power series in the strong coupling constant. We have indicated in Eq.(1.1) that the selected distribution should not be affected by non-perturbative corrections; we will return to this point below. We also note that inclusion of QCD corrections necessitates a clear definition of the renormalization scheme which then fixes the mass parameter extracted from the fit. Since the two popular choices of the renormalized mass parameter, the pole mass and the $\overline{\text{MS}}$ mass, differ by almost 7 GeV, the specification of the renormalization scheme in the extraction of the top quark mass is an important issue. Solving Eq.(1.1), we find the top quark mass m_t . In general, the quality of such solution depends on the *accuracy* of the theoretical prediction that we have in the right hand side which is controlled by the order in perturbation theory included there. It is well-known that *majority* of the analyses are performed with leading order theoretical tools. In general, this amounts to setting $T^{(1)} \rightarrow 0$ in the above equation. The expected error on m_t is then

$$\delta m_t \sim \frac{\alpha_s}{\pi} \frac{T^{(1)}}{T^{(0)'}} \sim \frac{\alpha_s m_t}{\pi} \frac{T^{(1)}}{T^{(0)}} \sim \frac{\alpha_s}{\pi} m_t \sim 6 \text{ GeV}, \quad (1.2)$$

where $T^{(0)'} = dT^{(0)}/dm_t$ and we used $T^{(0)'} \approx T^{(0)}/m_t$. It is obvious from Eq.(1.2) that the estimated error in Eq.(1.2) is *significantly larger* than the current $\mathcal{O}(1)$ GeV error on m_t . We conclude that if m_t is obtained from a generic distribution at leading order, one can not, in general, expect the accuracy that is better than few GeV. Fortunately, there are two ways to get around this problem. The first one requires inclusion of NLO QCD corrections into a theory prediction; effectively, this pushes the error to $m_t(\alpha_s/\pi)^2 \sim 0.3$ GeV which is acceptable. The second one amounts to finding a kinematic distribution which has a *strong* dependence on m_t ; in this case, $dT^{(0)}/dm \gg T^{(0)}/m_t$ and the estimate in Eq.(1.2) receives an additional suppression.

As we show below, *new* experimental techniques that address the question of the top quark mass determination follow the two approaches described above. Incidentally, the above discussion can be used to argue that *well-established* methods for the top quark mass determination may have additional systematic errors which are not accounted for in their error budgets. Indeed, the matrix element method² is designed to maximize probabilities for kinematics of observed events by adjusting values of the top quark mass on an event-by-event basis; it can be thought therefore as an attempt to fit a very large number of kinematic distributions for the best value of m_t .

An unsatisfactory feature of this methods is its “black-box” nature that does not allow one to understand which kinematic features of the top quark pair production process drive this sensitivity. While such methods

²The template method [11] is subject to similar arguments.

	Ref.[12]	Projections				
CM Energy	7 TeV	14 TeV				
Luminosity	$5fb^{-1}$	$100fb^{-1}$	$300fb^{-1}$	$300fb^{-1}$	$3000fb^{-1}$	
Pileup	9.3	19	30	19	30	95
Syst. (GeV)	0.95	0.7	0.7	0.6	0.6	0.6
Stat. (GeV)	0.43	0.04	0.04	0.03	0.03	0.01
Total, GeV	1.04	0.7	0.7	0.6	0.6	0.6

Table 1-1. Precision of the top quark mass measurements that can be expected using conventional (likelihood-type) methods. Extrapolations are based on the published CMS lepton-plus-jets analysis. An additional 0.3 GeV systematic error was added to all extrapolated results.

– by design – should find distributions that show strong dependence on m_t , it is not clear if the relevant distributions are sensitive to non-perturbative effects whose description from first principles is not possible. Moreover, such approaches routinely rely on the use of parton shower event generators instead of proper QCD theory. This means that Eq.(1.1) becomes

$$D = T(m_t, \alpha_s, \Lambda_{\text{QCD}}) \approx T_{\text{MC}}^{(0)}(m_t, \alpha_s, \Lambda_{\text{QCD}}, \text{tunes}), \quad (1.3)$$

114 where, as indicated in the last step, additional approximations, including parton shower tunes, are performed
 115 on the “theory” side. While the quality of this approximation *for the purpose of the top quark mass*
 116 *measurement* may be good, it is simply not clear how to assign the error to the parameter m_t which is
 117 extracted following this procedure. To make this problem explicit, the top quark mass extracted from
 118 Eq.(1.3) should be properly referred to as the “Monte-Carlo mass”, whose relation to m_t that enters the
 119 fundamental Standard Model Lagrangian is not understood.

120 In spite of the caveats with the top quark mass determination that are inherent to conventional methods, it
 121 is interesting to estimate precision in m_t that can be achieved at the LHC. We do that using extrapolations
 122 of what has been accomplished at the Tevatron and during the run I of the LHC. In Table 1-1 we show such
 123 projections for conventional methods assuming that the mass is measured in the lepton + jet channel for
 124 the 14 TeV LHC for different integrated luminosities and pile-up scenarios. We assume the $t\bar{t}$ production
 125 cross-section to be $\sigma_{pp \rightarrow t\bar{t}} = 167(951)$ pb at 7 and 14 TeV LHC, respectively. It follows from Table 1-1 that
 126 conventional methods may, eventually, lead to the measurement of the top quark mass with an error of about
 127 0.6 GeV and that this error is totally dominated by systematic uncertainties. It is interesting to point out
 128 that precision in m_t saturates for the integrated luminosity of 300 fb^{-1} and that there is no benefit of using
 129 yet higher luminosity for the top quark mass measurement. The reason for this is the increased pile-up and
 130 related degradation of the jet energy scale determination in the high-luminosity environment, see a detailed
 131 discussion in Section 1.7.1. Note, however, that the systematic error estimate in Table 1-1 includes 0.3 GeV
 132 that was added to all extrapolated results to account for unforeseen sources of systematics; without this
 133 0.3 GeV uncertainty, the error on the top quark mass measurement becomes very small.

134 Conceptual problems with conventional methods can be mitigated by measuring the top quark mass from
 135 well-defined kinematic distributions which, on the one hand, are sufficiently sensitive to m_t and, on the other
 136 hand, can be cleanly interpreted in terms of a particular type of the top quark mass. The latter requirement
 137 forces us to select kinematic distributions that are infra-red safe, so that their computations in higher-orders
 138 of QCD perturbation theory can be performed. In addition, methods for measuring the top quark mass
 139 should, ideally, be immune to contamination from beyond the Standard Model physics – a scenario that is

	Ref.[13]	Projections		
CM Energy	7 TeV	14 TeV		
Luminosity	$5fb^{-1}$	$100fb^{-1}$	$300fb^{-1}$	$3000fb^{-1}$
Syst. (GeV)	1.8	1.0	0.7	0.5
Stat. (GeV)	0.90	0.10	0.05	0.02
Total	2.0	1.0	0.7	0.5

Table 1-2. Projections for the uncertainty in m_t determined using the CMS end-point method [13]. Extrapolations are based on the published CMS analysis.

conceivable if there is top-like BSM physics at the energy scale close to $2m_t$. For example, if m_t is determined from the total cross-section $\sigma_{pp \rightarrow t\bar{t}}$ and if $pp \rightarrow t\bar{t}$ receives unknown contributions from top-like BSM physics, the extracted value of the top quark mass will be smaller than the true m_t . This scenario can occur for example in SUSY models with light stop squarks $m_{\tilde{t}} \sim m_t$ that are still not excluded experimentally (cf. discussion in Section 1.6.1).

Methods for top quark mass determination that are based on the analysis of kinematic distributions of top quark decay products are as close to an ideal method as possible. The main reason is that, up to small effects related to selection cuts and combinatorial backgrounds, kinematic variables involved in the analysis can often be chosen to be Lorentz invariant in which case they decouple the production stage from the decay stage. This minimizes impact of any physics, BSM or SM, related to $t\bar{t}$ production on the top quark mass measurement. Moreover, some of these methods are also insensitive to the physics of top quark decay and are entirely driven by energy-momentum conservation. We will describe two of the methods that belong to this category – the “end-point” method developed recently by the CMS collaboration [13] and the “ J/ψ ” method suggested long ago in Ref. [14].

The idea of the end-point method is based on the observation that the invariant mass distribution of a lepton and a b -jet contains a relatively sharp edge whose position is correlated with m_t . Therefore, by measuring the position of the end-point, one can determine the top quark mass. The number of events close to the end-point is fitted to a linear combination of a flat background and a linear function $N_{lb} \sim N_{\text{bck}} + S(m_{lb} - m_0)$; m_0 gives the position of the end-point. The attractive feature of this method is that it is (almost) independent of any assumption about the matrix element and that it clearly measures either the pole mass *or* some “kinematic” mass which is close to it. At the small expense of being more model-dependent, one can actually improve on this method by utilizing not *only* the position of the end-point but also the shape of the m_{lb} distribution. Note that away from the kinematic end-point the shape of m_{lb} distribution is accurately predicted through NLO QCD including off-resonance contributions and signal-background interferences [15, 16], while close to the end-point re-summed predictions are probably required and are not available at present.

Nevertheless, even without potential improvements, the end-point method offers an interesting alternative to conventional methods. Uncertainties in m_t that one may hope to achieve are estimated in Table 1-2. We note that by using the end-point method we *do gain in precision by going to high-luminosity LHC*. Our projections show that the error as small as 0.5 GeV can be reached. The dominant contribution to systematic uncertainty for each of these studies is the jet-energy scale and hadronization uncertainties. Similar to estimates of δm_t that can be achieved using conventional methods, we add 300 MeV to the systematic uncertainty in Table 1-2, to account for unforeseen sources of the systematics.

	Ref. analysis	Projections				
		14 TeV			33 TeV	100 TeV
CM Energy	8 TeV					
Luminosity	$20fb^{-1}$	$100fb^{-1}$	$300fb^{-1}$	$3000fb^{-1}$	$3000fb^{-1}$	$3000fb^{-1}$
Theory (GeV)	-	1.5	1.5	1.0	1.0	0.6
Stat. (GeV)	7.00	1.8	1.0	0.3	0.1	0.1
Total	-	2.3	1.8	1.1	1.0	0.6

Table 1-3. Extrapolations of uncertainties in top quark mass measurements that can be obtained with the J/Ψ method.

Another approach to measuring the top quark mass that is very different from conventional ones is the so-called J/ψ method [14]. Here the top quark mass is obtained from the invariant mass distribution of three leptons from the *exclusive* decay of the top quark $t \rightarrow eB \rightarrow eJ/\psi \rightarrow eee$. The extrapolations for the J/ψ -method are shown in Table 1-3. The attractive feature of this approach is its absolute complementarity to more traditional methods discussed above. The uncertainties in case of the J/ψ method are dominated by statistical uncertainties for luminosities below 100 fb^{-1} and by theory uncertainties for higher luminosities. The theory uncertainties in m_t are estimated to be of the order of 1 GeV; they are caused by scale and parton distribution functions uncertainties and by uncertainties in $b \rightarrow B$ fragmentation function. Some reduction of theory uncertainties can be expected, although dramatic improvements in our knowledge of the fragmentation function are not very likely. This is reflected in the change of the theory error shown in Table 1-3 for 14 TeV LHC with 3000 fb^{-1} where it is assumed that NNLO QCD computation of the exclusive production of J/ψ in $t\bar{t}$ events will become available and that the scale uncertainty will be reduced by a factor of two.

We note that other methods of measuring m_t with relatively high precision are possible and were, in fact, discussed in the literature. On the experimental side, the three-dimensional template fit method was recently presented by the ATLAS collaboration [17]. The key idea here is to determine the top quark mass, the light-quark jet energy scale and the b -quark jet energy scale from a simultaneous fit to data, thereby transforming a large part of the systematic uncertainty related to jet energy scales to a statistical one. The error on this measurement is not competitive with other m_t -determinations at the moment, but the key idea of the method can be applied in conjunction with other methods and will, hopefully, help to reduce systematic uncertainties. Another potentially interesting opportunity is provided by the top quark mass measurements based on exploiting m_t -dependence of lepton kinematic distributions. Although such studies were not actively pursued experimentally, they may offer an interesting avenue for the top quark mass measurement in the high-pile-up scenario given their independence of jet energy scale uncertainties. Theoretical studies of some lepton distributions and their sensitivity to m_t were performed through NLO QCD in Ref. [18] with the conclusion that $\mathcal{O}(1.5)$ GeV error on m_t can be achieved; further studies that include more realistic estimates of uncertainties are clearly warranted. Finally, it was proposed recently to employ $t\bar{t}j$ events to constrain the top quark mass [19]. This method is clean theoretically and appears to be feasibly experimentally; as shown in Ref. [19], the $\mathcal{O}(1)$ GeV uncertainty in m_t can be achieved.

The top quark width of 1.4 GeV is too narrow to be measured directly at the LHC. It can be probed indirectly through single top quark production [20], which can be determined to about 5%, see Section 1.3. The width can be measured directly to a few percent through a top pair threshold scan at a lepton collider [21, 7].

We conclude by making a general remark about the future of the top quark measurements at a hadron collider. While hadron collider measurements of the top quark mass *can not* compete with e^+e^- colliders,

our discussion shows that it is possible to have a number of top quark measurements at the LHC, including the high-luminosity option, which are clean theoretically and show high sensitivity to m_t . It is also important to stress that these measurements are typically limited by different types of uncertainties, so that combining their results under the assumption that errors are uncorrelated is a reasonable thing to do. A combination of the results of different measurements can lead to further reduction in the error on m_t that is achievable at the LHC, pushing it into a 0.3 – 0.4 GeV range. Further reduction of the uncertainty in the top quark mass determination is possible at suggested e^+e^- machines (ILC, CLIC, TLEP). Such measurements are important for testing if the Standard Model *without further extensions* can be consistently extrapolated to Planckian energy scales; interests in such studies should increase if no New Physics is found at the Run 2 at the LHC.

1.3 Top quark couplings

The couplings of the top quark to the W and Z bosons, photon, gluon, and the Higgs boson are explored in this Section. Simple estimates suggest that typical BSM physics at the TeV scale modifies the top quark couplings to gauge bosons at a few percent level [22] but, at the same time, larger $\mathcal{O}(10\%)$ shifts are still possible. Also, our knowledge of the top quark Yukawa coupling is poor at the moment and the direct measurement of this coupling with any precision is very important. Modifications of top quark couplings typically lead to a more complex structure of the interaction vertices which goes well beyond simple-minded re-scaling of SM couplings. This creates additional complications and requires us to understand how all the different couplings can be disentangled.

We note that most of the couplings are measured by comparing observed *rates* of relevant processes with SM expectations. This puts stringent requirements on theoretical predictions and experimental control of systematics making couplings measurements a difficult endeavor at the LHC. This Section compares the precision reach of couplings measurements at low-and high-luminosity LHC to lepton colliders (mainly ILC and CLIC). Higher-energy hadron colliders are not expected to improve the measurements much beyond the LHC sensitivity (except possibly for $t\bar{t}Z$) and are thus not studied here. The muon collider allows for the same studies as done at the ILC, but with smaller beam-related uncertainties and higher luminosity. TLEP provides larger data samples than the ILC; it has insufficient energy to measure Yukawa coupling through direct $t\bar{t}H$ production though it should be able to reach a sensitivity of $\mathcal{O}(30\%)$ to the $t\bar{t}H$ coupling from a threshold scan. The top quark couplings sensitivity is compared here using the anomalous coupling notation; a related discussion in terms of effective operators can be found in Refs. [23, 24].

1.3.1 Strong interaction

The strong coupling constant of the top quark is fixed in the Standard Model by the requirement of $SU(3)$ color gauge-invariance. The modifications of this coupling can be expected through radiative corrections which may introduce additional structures, such as chromoelectric and chromomagnetic dipole operators in $g\bar{t}t$ vertex, both in the Standard Model and in models of New Physics. For example, the Higgs exchange between top quarks modifies the strength of gluon-top quark interaction by $\mathcal{O}(0.5\%)$ while it does not affect the interaction of light quarks to gluons.

Strong interactions of the top quark are studied in top quark pair production, including the $t\bar{t}$ +jets processes, both at the Tevatron and the LHC. A summary of the current prediction and measurements is shown in Table 1-4. The experimental uncertainty of about 5% on $\sigma(pp \rightarrow t\bar{t})$ measurement is reached at the 8 TeV

LHC and it is not expected to significantly improve beyond that during further LHC operations. The theory prediction for the total cross-section through NNLO QCD is available [25, 26, 27]; it shows the residual scale uncertainty of about 3.5%, comparable to experimental precision. Note that at this level of precision electroweak corrections may be important; indeed, as shown in a recent update [28] the weak corrections to $t\bar{t}$ production at the LHC are close to -2.5% . We conclude that, at a few percent level, there is no indication that strong interactions of top quarks are significantly different from that of light quarks.

More exotic types of modifications of top quark strong interactions, such as chromoelectric d_t and chromomagnetic μ_t dipole moments of top quarks, are better constrained from changes in kinematic distributions, see Section 1.4. Ref. [29] finds that constraints of one percent or below are possible with 100 fb^{-1} at 13 TeV.

Exchanges of axiguons or Kaluza-Klein excitations of gluons not only modify couplings of top quarks to gluons, but also generate four-fermion operators that involve light and heavy quarks ($\bar{q}T^a q$) ($\bar{t}T^a t$). These operators can be directly probed at the LHC where the sensitivity to scales between 1.2 TeV and 3 TeV can be expected [30].

Finally, top quark coupling to gluons can be probed at a linear collider through a threshold scan. The peak cross-section at threshold is proportional to $\sigma_{\text{peak}} \sim \alpha_s^3/(m_t \Gamma_t)$. Using the total cross-section and other measurements at threshold, one can determine the strong coupling constant with better than one percent precision and the total width of the top quark Γ_t with the precision of a few percent [7, 6].

CM Energy [TeV] Luminosity [fb^{-1}]	Theory prediction		LHC Measurement	
	7	8	7 1-5	8 2-15
Top pairs $\sigma(t\bar{t})$ [pb]	172 ± 7 [25]	246 ± 10 [25]	173 ± 10 (LHC comb.) [32]	241 ± 32 (ATLAS) [31] 227 ± 15 (CMS) [33]
Single top $\sigma(\text{t-chan})$ [pb]			83 ± 20 (ATLAS) [34] 67 ± 6 (CMS) [36]	95 ± 18 (ATLAS) [35] 80 ± 13 (CMS) [37]
Single top $\sigma(Wt)$ [pb]	15.6 ± 1.2 [38]	22.2 ± 1.5 [38]	16.8 ± 5.7 (ATLAS) [39] 16 ± 4 (CMS) [40]	— 23.4 ± 5.4 (CMS) [41]

Table 1-4. LHC single top and top pair production cross section measurements.

1.3.2 Weak interactions: W boson

The coupling of the top quark to the W boson is studied in top quark decays and in single top quark production at the LHC and the Tevatron, and in top quark decays at the linear collider. The effective Lagrangian describing the Wtb interaction including operators up to dimension five is [23]

$$\mathcal{L} = -\frac{g}{\sqrt{2}}\bar{b}\gamma^\mu(V_L P_L + V_R P_R)tW_\mu^- - \frac{g}{\sqrt{2}}\bar{b}\frac{i\sigma^{\mu\nu}q_\nu}{M_W}(g_L P_L + g_R P_R)tW_\mu^- + h.c., \quad (1.4)$$

where M_W is the mass of the W boson, q_ν is its four-momentum, $P_{L,R} = (1 \mp \gamma_5)/2$ are the left- (right-) handed projection operators, and V_L is the left-handed coupling, which in the SM is equal to the Cabibbo-

269 Kobayashi-Maskawa matrix element V_{tb} [42]. The right-handed vector coupling V_R and the left- and right-
 270 handed tensor couplings g_L and g_R may only appear in the SM through radiative corrections.

271 The measurement of helicity fractions of W bosons through lepton angular distributions in top quark decays
 272 can distinguish SM-like left-handed vector couplings from right-handed vector and from left- or right-handed
 273 tensor couplings. With the data collected at 8 TeV LHC, V_R , g_L and g_R can be constrained to be smaller
 274 than 0.1. We note that theoretical predictions for W -boson helicity fractions in the SM have been extended
 275 to NNLO QCD [43, 44, 45] and, therefore, theory uncertainties on helicity fractions are about one order
 276 of magnitude smaller than experimental one. Measuring the helicity fraction to a similar level at the high-
 277 luminosity LHC and beyond is therefore necessary to obtain the best sensitivity to new physics.

278 Single top quark production involves the tWb vertex in top quark production and thus also provides
 279 information on the magnitude of the tWb coupling and the CKM matrix element $|V_{tb}|$. Single top quarks
 280 are produced in three different modes: the “ t -channel” mode which has the largest cross section, the “ Wt
 281 associated production” mode with the next-to-largest cross section, and the “ s -channel” production mode
 282 which has a very small cross section. The LHC cross section measurements for t -channel and Wt together
 283 with the corresponding prediction are shown in Table 1-4. The three modes have different sensitivities to new
 284 physics and anomalous couplings. LHC measurements of single top quark production, in particular in the
 285 t -channel mode, are also sensitive to off-diagonal CKM matrix elements [46]. The single top production cross
 286 section measurement is dominated by systematic uncertainties already in the current dataset [34, 36, 39], and
 287 the situation is not expected to improve much at higher energies or with larger datasets. The ultimate cross
 288 section uncertainty will likely be around 5%, similar to top pair production, so that uncertainties on tWb
 289 coupling and $|V_{tb}|$ will be close to 2.5% [47]. Searches for anomalous couplings in the tWb vertex depend on
 290 the ability to separate the signal from backgrounds and are less limited by systematic uncertainties. A search
 291 for CP violation through an anomalous coupling gives a limit on $Im(g_R)$ [48]. Finally, an extrapolation of
 292 the sensitivity to anomalous couplings from single top quark production and decay shows that with 300 fb^{-1}
 293 the anomalous couplings as small as 0.01 can be probed.

294 Electron-positron colliders are expected to do a comparable job in exploring the strength of tWb interaction
 295 vertex by considering the cross-section scan of σ_{tbW} cross-section at CM energies between m_t and $2m_t$. It
 296 was estimated in Ref. [22] that g_{tWb} can be measured with the precision of about two percent. Among more
 297 exotic options is the possibility to study tWb interaction at a γe collider, with a reach of 10^{-1} to 10^{-2} [49].
 298 The reach is about 10^{-3} to 10^{-2} for a LHC-based electron-proton collider with a CM energy of 1.3 TeV [50].

299 Knowledge of tWb interaction can be used to compute the top quark decay width of the Standard Model
 300 but a direct measurement of Γ_t is also of interest, see Section 1.2.

301 1.3.3 Electroweak interaction: Z boson and photon

302 The interaction of the top quark with neutral electroweak gauge bosons has not been studied in detail so far.
 303 Indeed, although both the charge of the top quark [51] and the production cross-section of top pair in asso-
 304 ciation with a photon were measured experimentally [52], this does not give us all the information required
 305 to fully constrain the $t\bar{t}\gamma$ vertex. The interaction of top quarks with the Z boson has not been measured yet.
 306 Similarly to other coupling, a measurement with $\mathcal{O}(10\%)$ precision will be useful for constraining models of
 307 physics beyond the Standard Model. It is challenging, but perhaps not impossible, to probe $t\bar{t}Z$ and $t\bar{t}\gamma$
 308 couplings at the LHC with that precision, while a lepton collider can easily do that.

A general expression for $t\bar{t}V$, $V = \gamma, Z$ interaction vertex is [22]

$$\Gamma_{\mu}^{ttX} = ie \left\{ -\gamma_{\mu} ((F_{1V}^X + F_{2V}^X) + \gamma_5 F_{1A}^X) + \frac{(q - \bar{q})_{\mu}}{2m_t} (F_{2V}^X - i\gamma_5 F_{2A}^X) \right\},$$

where X is either a photon ($X = \gamma$) or Z boson ($X = Z$). The couplings F_{1V}^{γ} , F_{1V}^Z and F_{1A}^Z have tree-level SM values.

The LHC experiments have measured the production of photons in association with top quark pairs, and will measure both the $\gamma + t\bar{t}$ and $Z + t\bar{t}$ cross sections. However, in both cases, significant kinematic cuts on final state particles are required to either suppress the backgrounds or, in case of photons, select events where photons are emitted from top quarks rather than from their decay products [53, 54, 22]. Therefore, extracting the top-photon or top- Z coupling from the associated production is difficult; it relies on a detailed theoretical understanding of the production process which is becoming available thanks to recent studies of $pp \rightarrow t\bar{t}\gamma$ and $pp \rightarrow t\bar{t}Z$ processes in next-to-leading order in QCD [55, 56, 57, 58]. Single top quark production in association with a Z boson can also be used to study the tZ coupling [59].

Measurements of the $t\bar{t}\gamma$ and $t\bar{t}Z$ couplings with the highest precision can be performed at a linear collider [21]. The two couplings are entangled in the top pair production process. Separating the two couplings requires polarized beams. For the projections in Table 1-5, electron and positron polarizations of 80% and 30%, respectively, are assumed. It follows from Table 1-5 that most of the top quark couplings to the photon and the Z boson can be measured at a linear collider (ILC/CLIC) to a precision that is typically an order of magnitude better than at the LHC. The precision on the combined coupling accessible at TLEP should be even better than that at the linear collider due to the higher integrated luminosity. However, a lack of beam polarization makes it challenging to disentangle the γ and Z couplings. A muon collider provides larger integrated luminosity and smaller beam uncertainties but also challenging backgrounds; thus it is not clear if it will be able to improve on the linear collider measurements.

In summary, although a linear collider will achieve the highest precision in the $t\bar{t}Z$ and $t\bar{t}\gamma$ coupling measurements, it is clear that the LHC – and in particular its high-luminosity phase – will be able to probe these couplings in an interesting precision range where deviations due to generic BSM physics are expected.

1.3.4 Yukawa coupling

The coupling of the top quark to the Higgs boson is of great interest. Since the top quark provides one of the largest contributions to the mass shift of the Higgs boson, any deviation in the $t\bar{t}H$ coupling from its Standard Model value may have far-reaching consequences for the naturalness problem. The coupling of the top quark to the Higgs boson can be measured at the LHC in different final states. It will also be studied in detail at lepton colliders. More details on the top Yukawa coupling measurements can be found in the Higgs working group chapter of this report.

The process $pp \rightarrow t\bar{t}H$ can be studied in a variety of final states, depending on the top quark decay mode (lepton+jets or dilepton or all-jets) and the Higgs decay mode ($b\bar{b}$, $\gamma\gamma$, WW etc.). Each final state has a its own, typically large background, mainly from top quark pair production in association with jets or electroweak bosons. The coupling of the top quark to the Higgs boson is extracted from these measurements with relatively large uncertainties of about twenty percent initially, with an improvement to ten percent at

Collider	LHC		ILC/CLIC
	14	14	
CM Energy [TeV]	14	14	0.5
Luminosity [fb^{-1}]	300	3000	500
SM Couplings			
photon, F_{1V}^γ (0.666)	0.042	0.014	0.002
Z boson, F_{1V}^Z (0.24)	0.50	0.17	0.003
Z boson, F_{1A}^Z (0.6)	0.058	?	0.005
Non-SM couplings			
photon, F_{1A}^γ	0.05	?	?
photon, F_{2V}^γ	0.037	0.025	0.003
photon, F_{2A}^γ	0.017	0.011	0.007
Z boson, F_{2V}^Z	0.25	0.17	0.006
Z boson, ReF_{2A}^Z	0.35	0.25	0.008
Z boson, ImF_{2A}^Z	0.035	0.025	0.015

Table 1-5. Expected precision of the top quark coupling measurements to the photon and the Z boson at the LHC [30] and the linear collider [21]. Expected magnitude of such couplings in the SM is shown in brackets. Note that the “non-standard model” couplings appear in the Standard Model through radiative corrections; their expected magnitude, therefore, is 10^{-2} .

the high-luminosity LHC [60, 61, 30]. At the high-luminosity LHC, the $t\bar{t}H$ final state is also a promising channel to measure the muon coupling of the Higgs boson [62].

Better precision in the top-Higgs coupling can be achieved at lepton colliders running at a sufficiently high CM energy and collecting large integrated luminosity. Initial studies focused on a CM energy of 800 GeV where the $t\bar{t}H$ cross section is largest, however a measurement at 500 GeV is also possible. For the projections in Tab. 1-6, electron and positron polarizations of 80% and 30%, respectively, are used. For the ILC/CLIC, a luminosity of twice the ILC design luminosity is assumed. A comparison of the top Yukawa coupling precision expected at different colliders is shown in Table 1-6, from where it follows that a linear collider provides marginal improvements compared to the high-luminosity LHC. It is also possible to measure the Yukawa coupling in a threshold scan that is sensitive to the modification of the $t\bar{t}$ production cross-section through a Higgs exchange. A precision of $\mathcal{O}(30)\%$ can, perhaps, be achieved in this case. Note that this is the only way to get information on the top Yukawa coupling at TLEP.

1.4 Kinematics of top-like final states

Working with top quarks requires us to understand how they are produced and how they decay. In this Section, we discuss what we know about that and what we can learn in the future. While such a discussion is interesting in its own right, it also allows us to understand to what extent deviations from expected behavior of various top quark distributions in different kinematic regimes can be probed at existing and future facilities. In general, after the run I of the LHC and the studies of top quark pair production at the Tevatron, it is fair to say that dynamics of $t\bar{t}$ production is well-understood. The only, but significant, discrepancy that exists is the disagreement between forward-backward asymmetry for top quarks expected in

Collider	LHC		ILC	ILC	CLIC
CM Energy [TeV]	14	14	0.5	1.0	1.4
Luminosity [fb^{-1}]	300	3000	1000	1000	1000
Top Yukawa coupling κ_t	(20 – 25)%	(8 – 20)%	10%	4%	4%

Table 1-6. Expected precision of the top quark Yukawa coupling measurement expected at the LHC and the linear collider [21]. The range for the LHC precision corresponds to an optimistic scenario where systematic uncertainties are scaled by 1/2 and a conservative scenario where systematic uncertainties remain at the 2013 level [60, 61]. The ILC [21, 63] and CLIC [64] projections assume polarized beams and nominal integrated luminosities.

366 the Standard Model and the measured value of this asymmetry at the Tevatron. Is it possible to clarify the
 367 situation with forward-backward asymmetry at the LHC or other future facilities? This is a data-motivated
 368 question that we address in this Section.

369 1.4.1 Kinematic distributions in top quark pair production

370 Our current understanding of top quark pair production in hadron collisions is based on next-to-leading
 371 order computations for fully-differential process $pp \rightarrow t\bar{t} \rightarrow W^+W^-b\bar{b}$ both within and beyond the narrow
 372 width approximation [15, 16, 65, 66]. The comparison of these computations ensures that the narrow
 373 width approximation works very well at the LHC unless one moves to extreme kinematic regimes where
 374 production of two on-shell top quarks becomes kinematically unfavorable. The success of the narrow
 375 width approximation in $t\bar{t}$ production allows us to claim its validity for more complicated processes such as
 376 production of top quark pairs in association with jets [67, 68, 69]. or gauge bosons, that we will discuss
 377 in the next Section. Existing theoretical results on top quark pair production will be further improved by
 378 extending available results for differential quantities to next-to-next-to-leading order in perturbative QCD.
 379 We note that such results for the total cross-section $pp \rightarrow t\bar{t}$ were recently obtained [25, 26, 27].

380 We will now take a closer look at the quality of theoretical description of various kinematic distributions.
 381 To this end, we show distributions in the top quark transverse momentum p_\perp in $pp \rightarrow t\bar{t}$ at the 14 TeV
 382 LHC in Fig. 1.4.1 and indicate the uncertainties in the predictions caused by imperfect knowledge of parton
 383 distribution functions and missing higher-order corrections that we estimate by varying renormalization and
 384 factorization scales by a factor of two around the fixed value $\mu = m_t$. The computations are performed with
 385 MCFM [70]. We see that scale uncertainties dominate and that uncertainties in theory predictions are at
 386 the level of twenty percent.

387 Another interesting kinematic regime is the boosted one and, as we will see, it is more difficult to understand
 388 the uncertainty in the theoretical prediction for this quantity. Indeed, a MCFM-based computation shows
 389 that for $p_\perp > 800$ GeV, the uncertainties on rapidity and p_\perp distributions roughly double compared to
 390 the non-boosted regime [71]. However, these uncertainties may be underestimated. Indeed, resummation
 391 computations, either traditional or SCET-based³, point towards additional positive contributions to p_\perp
 392 distributions at high values of the top quark momentum [72, 73]. Forthcoming NNLO computations will be
 393 required to resolve this issue.

³SCET refers to Soft-Collinear Effective Field Theory.

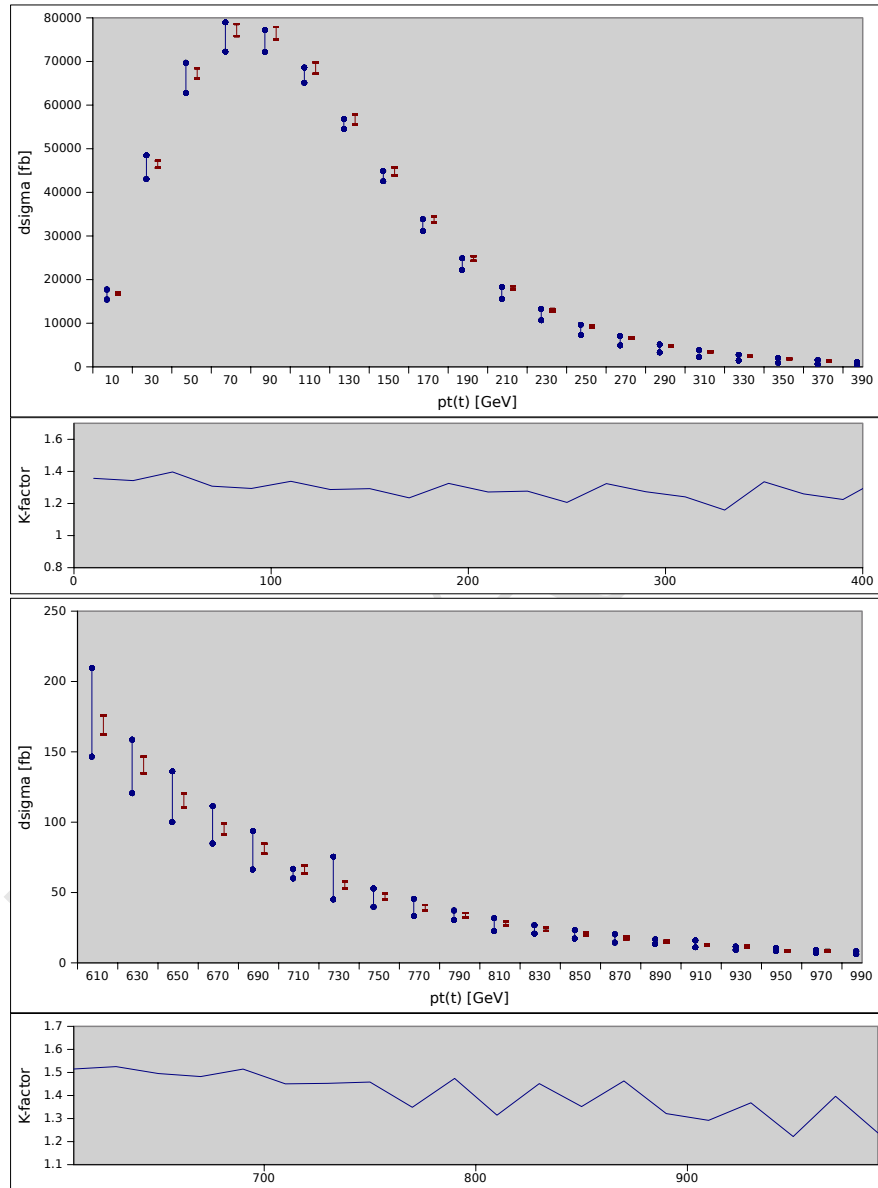


Figure 1-2. NLO QCD predictions [70] for the transverse momentum of the top quark at the 14 TeV LHC. Blue error bars correspond to scale variation by a factor of two around $\mu = m_t$. Dark red error bands correspond to variation of different MSTW pdf error sets.

394 In general, all kinematic distributions in top quark pair production are routinely checked for signs of new
 395 physics. Prominent among them is the distribution in the invariant mass of a $t\bar{t}$ pair which may be
 396 significantly modified by the presence of resonances that decay to top pairs. Theoretical predictions for
 397 such distributions exist both in fixed order QCD and in SCET [72]; they show theoretical errors between ten
 398 and fifteen percent, depending on $m_{t\bar{t}}$ and, similar to p_{\perp} distribution, significant differences between fixed
 399 order and resummed results at large values of $m_{t\bar{t}}$.

400 Other kinematic distributions, such as angular correlations between either top quarks or their decay products,
 401 did not lead to conclusive studies at the Tevatron because of low statistics. However, such studies at the LHC
 402 will become increasingly important as the tool to analyze various subtle features of top quark interactions
 403 with with both SM and, hopefully, BSM particles. In the following subsections we discuss examples of this,
 404 the top quark spin correlations and the forward-backward $t\bar{t}$ asymmetry.

405 1.4.2 Top quark spin correlations

406 Spin correlations between t and \bar{t} are an interesting feature of top quark physics, related to the fact that
 407 top quark lifetime is so short that $t(\bar{t})$ spin information is transferred to their decay products without being
 408 affected by non-perturbative hadronization effects. Observable spin correlations are affected by the structure
 409 of $g\bar{t}t$ and tWb interaction vertices. After the observation of top quark spin correlations at the Tevatron [74]
 410 and recently at the LHC [75, 76], experimental analyses will soon be able to probe spin correlations in detail
 411 and, perhaps, use spin correlations as an analysis tool to find and constrain physics beyond the Standard
 412 Model.

413 The cleanest $t\bar{t}$ samples to study spin correlations are the ones with two opposite-sign leptons in the final
 414 state. Spin correlations in this dilepton mode manifest themselves most prominently in the distribution
 415 of the relative azimuthal angle between the two leptons [77]. This distribution is robust under higher
 416 order corrections and parton showering effects [65, 78, 79]. For standard acceptance cuts, NLO QCD
 417 effects introduce shape changes of at most twenty percent. If additional cuts are applied that enhance spin
 418 correlations, NLO corrections increase the correlation even further. Electroweak corrections have negligible
 419 effects and scale variations are small because distributions are typically normalized. On the experimental
 420 side, the reconstruction of the lepton opening angle in the laboratory frame is straightforward and can be
 421 done with small systematic uncertainties. The normalized azimuthal opening angle distribution is therefore
 422 an ideal observable for studying top quark spin correlations. Of course, other observables such as helicity
 423 angles, double differential distributions and asymmetries can also be explored.

424 The utility of top quark spin correlations to search for physics beyond the Standard Model stems from the
 425 vector coupling of top quarks to gluons, from the fermion nature of the top quark, and its decay into a
 426 W boson and a b quark through a left-handed vector current; any changes in that list must lead to an
 427 observable change in the spin correlation pattern. For example, it has been shown that top quark spin
 428 correlations can be used to distinguish SM top quarks from scalar partners (stops) even if tops and stop are
 429 degenerate in mass [80]. The potential of spin correlations to distinguish SM top pair production and stop
 430 ($m_{\bar{t}} = 200$ GeV) pair production is illustrated in Fig. 1-3 [71].

431 Modifications of $g\bar{t}t$ vertex, that can be parametrized in terms of top quark chromomagnetic $\hat{\mu}_t$ and electric
 432 \hat{d}_t dipole moments, can be exposed through spin correlations in the dileptonic and in the semileptonic
 433 channels [29, 81]. Indeed, using dilepton events sample of the 20 fb^{-1} run at 8 TeV, it should be possible
 434 to constrain $\text{Re}(\hat{\mu}_t)$ and $\text{Re}(\hat{d}_t)$ at the few percent level. The imaginary parts $\text{Im}(\hat{\mu}_t)$ and $\text{Im}(\hat{d}_t)$ can be
 435 constrained with 15–20 percent precision from lepton-top helicity angles in the semileptonic channel where a
 436 full reconstruction of the $t\bar{t}$ system is possible, using the same dataset. Ref. [29] finds that constraints at the

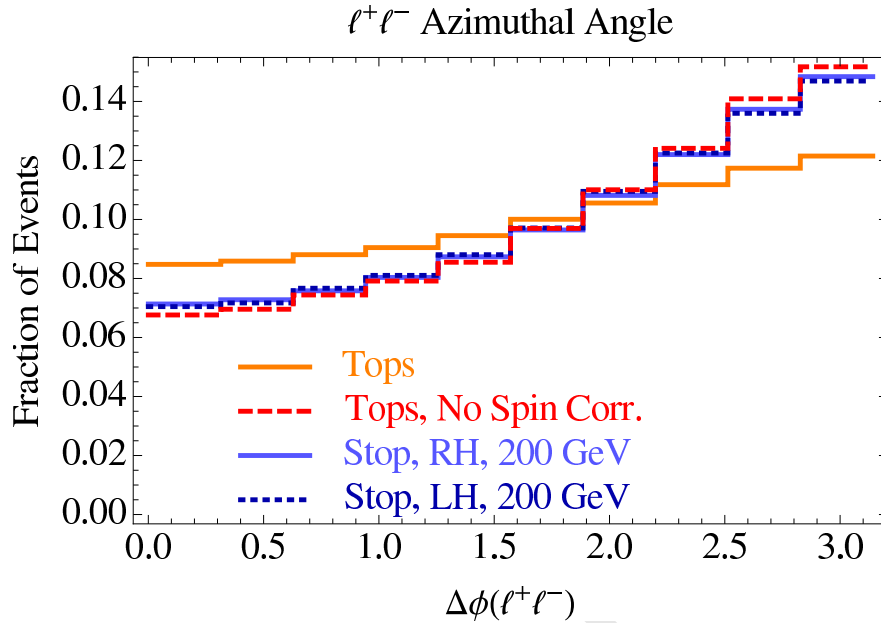


Figure 1-3. Top quark spin correlation angle for top quark production in the SM and without spin correlation and for stop quark production with different couplings [71].

437 level of one percent or even below are possible with 100 fb^{-1} at 13 TeV. Finally, in case of the discovery of a
 438 new resonances which decays into $t\bar{t}$ pairs, top quark spin correlations can also be used to analyze couplings
 439 of this new particle [82, 83].

440 1.4.3 Top quark pair forward-backward asymmetry

Top quark pair production in $q\bar{q}$ collisions exhibits forward-backward asymmetry that arises in higher orders in perturbative QCD [84, 85, 86, 87, 88]. As the result, the top quark is preferentially emitted in the direction of the incoming quark, while the anti-top quark follows the direction of the incoming antiquark. At the Tevatron, the direction of the incoming quark corresponds to the direction of the incoming proton, while the incoming anti-quark most likely comes from an anti-proton. Since LHC is a proton-proton collider, the $t\bar{t}$ asymmetry observation becomes difficult because directions of quark and anti-quark are not correlated with directions of initial hadrons and, in addition, there is a large gluon flux that reduces the asymmetry. The forward-backward asymmetry at the LHC is measured through the difference in rapidity distributions of t and \bar{t} ; harder spectrum of valence quarks in the proton and correlation of top quark direction with the direction of the incoming quark make top rapidity distribution broader than the rapidity distribution of anti-tops. The corresponding asymmetry is referred to as the charge asymmetry. It can be written as

$$A_C^\eta = \frac{N(\Delta|\eta| > 0) - N(\Delta|\eta| < 0)}{N(\Delta|\eta| > 0) + N(\Delta|\eta| < 0)} \quad (1.5)$$

441 where $\Delta|\eta| \equiv |\eta_t| - |\eta_{\bar{t}}|$ tells us whether the reconstructed top or anti-top is more central according to
 442 lab-frame *pseudo-rapidity*.

443 Inclusive forward-backward asymmetries measured at the Tevatron exceed SM predictions by almost three
 444 standard deviations [89, 90], with stronger dependence on $t\bar{t}$ invariant mass and rapidity than predicted by

445 the SM. At the LHC, the ATLAS and CMS Collaborations have performed measurements of the charge
 446 asymmetry A_C [91, 92] and found agreement with SM predictions although measurements have large errors
 447 that makes them not conclusive.

448 Given that the forward-backward asymmetry is the *only* measurement in top physics that shows profound
 449 disagreement with the Standard Model prediction, we feel it is important to understand if this problem can
 450 be resolved. Our estimates for the LHC are presented below. At a linear collider, it is not possible to address
 451 this problem directly unless the asymmetry mediator is light and can be directly studied in $e^+e^- \rightarrow t\bar{t}jj$.

452 The higher energy of the 14 TeV LHC increases the fraction of $t\bar{t}$ events that arise from gluon fusion, relative
 453 to 7 and 8 TeV LHC. Since $gg \rightarrow t\bar{t}$ does not produce an asymmetry, the asymmetric signal decreases with
 454 increased center of mass energy of the collider. Already at 7 TeV LHC measurements of the top charge
 455 asymmetry are limited by systematic uncertainties and the situation will not improve at a higher-energy
 456 machine.

457 SM predictions for 14 TeV LHC as a function of cuts on minimum invariant mass of the top pair $m_{t\bar{t}}$ is
 458 calculated in Ref. [93]. Cutting on either $t\bar{t}$ invariant mass or center-of-mass rapidity increases the proportion
 459 of $q\bar{q}$ -initiated top pair events relative to gluon-initiated events, and thus enhances the signal. However, even
 460 with kinematic cuts, the size of the signal at the 14 TeV LHC is comparable to the systematic uncertainties on
 461 the current measurements. The dominant contributions to the systematic errors are jet energy scale, lepton
 462 identification, background modeling ($t\bar{t}$, W + jets, multijets), and model dependence of signal generation
 463 and the unfolding procedure. Several contributions to systematic errors, such as jet energy scale and lepton
 464 identification, can be reduced with increased luminosity. Possible improvements in background modeling are
 465 less clear. The dilepton channel can also be used, usually by defining a lepton-based asymmetry rather than
 466 the top quark based A_C , with a sensitivity similar to the lepton+jets one [94, 95].

467 Our estimates of the ultimate LHC sensitivity [71] show that with sufficient luminosity, the 14 TEV LHC
 468 will be able to *conclusively* measure the SM asymmetry provided that largest systematic errors identified
 469 in current ATLAS and CMS measurements⁴ scale with luminosity. If the asymmetry is enhanced due to
 470 BSM effects – as indicated by the Tevatron data – the prospects for observing the asymmetry by CMS and
 471 ATLAS become event brighter.

472 We note that internal study of LHCb collaboration [96] concludes that a measurement of the SM $t\bar{t}$ asymmetry
 473 by LHCb experiment is possible at the 14 TeV LHC with sufficient luminosity, as suggested earlier in Ref.[97].
 474 This will provide a measurement of A_c at the LHC which is complementary to the measurement of A_c by
 475 ATLAS and CMS collaborations. Combining all the measurements, one can probably achieve a significant
 476 improvement in the precision of these measurements compared to individual experiments and hopefully solve
 477 the forward-backward asymmetry puzzle.

478 To this end, note that out of the vast zoology of proposed BSM explanations for the Tevatron anomaly in the
 479 top forward-backward asymmetry, axigluons [98, 99, 100] are left looking most plausible after the low-energy
 480 LHC run has been completed. Detailed discussions of experimental constraints on axigluon models can be
 481 found in [101] for “light” ($M_{G'} < 450$ GeV) axigluons and in [102] for heavy axigluons. The high-luminosity
 482 LHC should be able to rule out axigluon models currently under consideration, though it is possible to come
 483 up with models that explain the Tevatron asymmetry and are difficult to probe at the LHC.

⁴ According to CMS estimates [92], the major contributions to systematic uncertainty are background modeling (40%),
 lepton identification (30%) and W + jets modeling (13%).

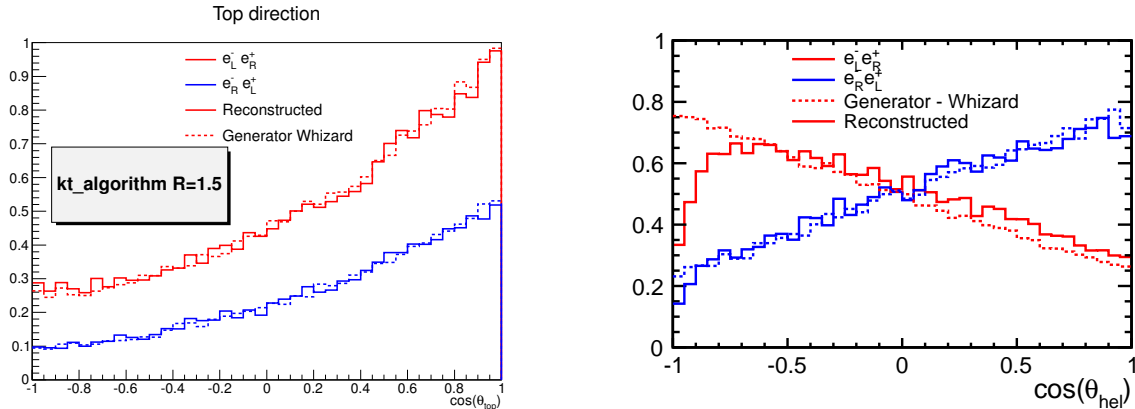


Figure 1-4. *Left:* Reconstructed forward backward asymmetry compared with the prediction by the event generator WHIZARD [107, 108]. *Right:* Polar angle of the decay lepton in the rest frame of the t quark.

1.4.4 Other kinematic observables related to A_{FB} at the LHC

It is interesting to point out that A_{FB} asymmetry is one of many angular variables whose distributions can be measured in hadron collisions. Indeed, if we consider $t\bar{t}$ production in parton collisions in semileptonic mode, in principle, the full kinematics of the event is characterized by 12 angles and the center-of-mass partonic collision energy. In principle, kinematic distributions in these angles describe all kinematic correlations in $t\bar{t}$ events and therefore are sensitive to potential deviations of top couplings to $q\bar{q}$ or gg initial states from their Standard Model values. The forward-backward asymmetry provides an example of this more general framework.

It will be certainly worthwhile to pursue full angular analysis to understand subtle aspects of top quark pair production or even processes with additional radiation, e.g. $t\bar{t}j$, especially in the context of studying top quark couplings to other Standard Model particles, discussed in Section 1.3. Unfortunately, this general analysis was not attempted so far. Here, we illustrate this general idea by mentioning additional kinematic observables that can be explored. For example, Refs. [103, 104] introduce two type of additional asymmetries in $t\bar{t}j$ events that can be used to either probe the charge asymmetry or energy asymmetry in a complementary way or, e.g., provide additional tools to measure the qg contribution to $t\bar{t}$ production.

1.4.5 Kinematics at the linear collider

At a linear collider, observables such as A_{FB}^t or the slope of the helicity angle λ_t [105] are sensitive to the chiral structure of the $t\bar{t}X$ vertex. A result of a full simulation study of semileptonic $t\bar{t}$ decays [106] is shown in Fig. 1-4.

It demonstrates that it will be possible to measure both the production angle θ_{top} of the t quark and the helicity angle θ_{hel} to great precision over a large range, leading to measurements of A_{FB}^t and λ_t with a precision of about 2%. Additionally, the A_{FB}^t and other measurements of the $t\bar{t}$ system, will benefit from a $> 60\%$ pure sample [109] in which to measure the b quark charge. The chiral structures of couplings can be possibly be probed in this way.

508 Since a significant fraction of top studies will be around the $t\bar{t}$ threshold, understanding kinematic distribu-
509 tions of top quark decay products in this region is important. This is a non-trivial problem that is affected
510 by the need to account for QCD Coulomb interactions to all orders. While results for the total threshold
511 cross-section $e^+e^- \rightarrow t\bar{t}$ are currently known through NNLO in QCD [110], similar accuracy for kinematic
512 distributions has not been achieved and it is an interesting and important problem to pursue in the future,
513 if the potential of the threshold scan at the LHC is to be fully exploited.

514 1.5 Rare decays

515 1.5.1 Introduction

516 Extensions of the SM often induce sizable flavor-violating couplings between the top quark and other
517 Standard Model particles, typically through new physics (NP) in loops. In contrast, flavor-changing neutral
518 couplings of the top are highly suppressed in the SM, so that the measurement of anomalous or flavor-
519 violating couplings of the top quark provides a sensitive probe of physics beyond the Standard Model. Since
520 the top quark decays before hadronizing, top flavor violation is ideally probed through direct flavor-changing
521 neutral current (FCNC) production and decays of the top quark in experiments at the energy frontier.
522 Although flavor-violating couplings of the top may arise from many sources, if the responsible NP is heavier
523 than the top, it can be integrated out and its effects described by an effective Lagrangian: for details, see,
524 for example, [111].

525 In Section 1.5.2 we summarize predictions for the size of flavor-changing top decays in the Standard Model
526 and in various motivated models for new physics. In Section 1.5.3 we collect the current best limits on top
527 FCNC decays from direct searches. In Section 1.5.4 we investigate the potential for future measurements at
528 the LHC and ILC to constrain top FCNC.

529 1.5.2 Flavor-violating Top Decays

530 The branching ratio (BR) of a flavor-violating decay of the top quark is given by the ratio of the flavor-
531 violating partial width relative to the dominant top quark partial width, $\Gamma(t \rightarrow bW)$. In Table 1-7 we
532 summarize predictions for top FCNC BRs in the Standard Model and various motivated NP models. In the
533 case of NP, the listed BR is intended as an approximate maximal value given ancillary direct and indirect
534 constraints.

535 1.5.2.1 SM top FCNC

536 SM contributions to top FCNC are necessarily small, suppressed by both the GIM mechanism and by the
537 large total width of the top quark due to the dominant mode $t \rightarrow bW$ [120, 121]. This essentially guarantees
538 that any measurable branching ratio for top FCNC decays is an indication of NP. The values in Table 1-7
539 are from the updated numerical evaluation in reference [112]. Note that the results are very sensitive to the
540 value of m_b as they scale as $m_b(m_t)^4$. The difference between decays involving u quark and c quarks arises
541 from the relative factor $|V_{ub}/V_{cb}|^2$.

Table 1-7. SM and NP predictions for branching ratios of top FCNC decays. The SM predictions are taken from [112], on 2HDM with flavor violating Yukawa couplings [112, 113] (2HDM (FV) column), the 2HDM flavor conserving (FC) case from [114], the MSSM with 1 TeV squarks and gluinos from [115], the MSSM for the R -parity violating case from [116, 117], and warped extra dimensions (RS) from [118, 119].

Process	SM	2HDM(FV)	2HDM(FC)	MSSM	RPV	RS
$t \rightarrow Zu$	7×10^{-17}	–	–	$\leq 10^{-7}$	$\leq 10^{-6}$	–
$t \rightarrow Zc$	1×10^{-14}	$\leq 10^{-6}$	$\leq 10^{-10}$	$\leq 10^{-7}$	$\leq 10^{-6}$	$\leq 10^{-5}$
$t \rightarrow gu$	4×10^{-14}	–	–	$\leq 10^{-7}$	$\leq 10^{-6}$	–
$t \rightarrow gc$	5×10^{-12}	$\leq 10^{-4}$	$\leq 10^{-8}$	$\leq 10^{-7}$	$\leq 10^{-6}$	$\leq 10^{-10}$
$t \rightarrow \gamma u$	4×10^{-16}	–	–	$\leq 10^{-8}$	$\leq 10^{-9}$	–
$t \rightarrow \gamma c$	5×10^{-14}	$\leq 10^{-7}$	$\leq 10^{-9}$	$\leq 10^{-8}$	$\leq 10^{-9}$	$\leq 10^{-9}$
$t \rightarrow hu$	2×10^{-17}	6×10^{-6}	–	$\leq 10^{-5}$	$\leq 10^{-9}$	–
$t \rightarrow hc$	3×10^{-15}	2×10^{-3}	$\leq 10^{-5}$	$\leq 10^{-5}$	$\leq 10^{-9}$	$\leq 10^{-4}$

542 1.5.2.2 BSM top FCNC

543 Many models for new physics predict new contributions to top FCNC that are orders of magnitude in excess
544 of SM expectations. Extended electroweak symmetry breaking sectors with two Higgs doublets (2HDM)
545 lead to potentially measurable FCNC. Parametric expectations are particularly large for 2HDM with tree-
546 level flavor violation, for which flavor-violating couplings between Standard Model fermions and the heavy
547 scalar Higgs H or pseudoscalar A are typically posited to scale with quark masses, $\propto \sqrt{m_q m_t / m_W^2}$, in order
548 to remain consistent with limits on light quark FCNCs. Estimates in Table 1-7 are taken from references
549 [122, 113]. The flavor-violating decays arise at one loop due to the exchange of H , A , and the charged Higgs
550 scalar H^\pm , with the rate that depends on both the tree-level flavor-violating couplings between fermions and
551 the heavy Higgs bosons and the masses of the heavy Higgs bosons themselves.

552 Even 2HDM with tree-level flavor conservation guaranteed by discrete symmetries predicts measurable top
553 FCNC due to loop processes that involve the additional charged Higgs bosons. In this case the rate for
554 flavor-violating processes depends on the mass of the charged Higgs and the angle $\tan \beta$ parameterizing the
555 distribution of vacuum expectation values between the two Higgs doublets. In Type-I 2HDM, the branching
556 ratios are typically small; the most promising candidate is $t \rightarrow gc \sim 10^{-8}$, with rates for $t \rightarrow hq$ several
557 orders of magnitude smaller. In Type-II 2HDM, the leading contribution to $t \rightarrow hq$ is enhanced by $\mathcal{O}(\tan^4 \beta)$
558 and may be considerable at large $\tan \beta$. The most optimistic cases are presented in Table 1-7, taken from
559 [114] for Type I and Type II 2HDM. However, given that Higgs coupling measurements now constrain the
560 allowed range of mixing angles in these 2HDM, the maximal rates for $t \rightarrow hq$ consistent with ancillary
561 measurements are likely smaller.

562 In the MSSM, top FCNC arise at one loop in the presence of flavor-violating mixing in the soft mass
563 matrices. Flavor violation involving the stops is much more weakly constrained by indirect measurements
564 than flavor violation involving light squarks (particularly in the down-squark sector), allowing for potentially
565 large mixing. However, rapidly-advancing limits on direct sparticle production have pushed the mass scale
566 of squarks and gluinos to ≥ 1 TeV, suppressing loop-induced branching ratios. To obtain realistic estimates,
567 in Table 1-7 we extrapolate the results of [115] to the case of $m_{\tilde{g}} \sim m_{\tilde{q}} = 1$ TeV. If R -parity is violated in
568 the MSSM, top decays may also be induced at one loop by baryon (B) or lepton (L) number-violating RPV
569 couplings, though B -violating couplings dominate by an order of magnitude or more. For the estimates in

570 Table 1-7, we extrapolate the results of [116, 117] to $m_{\tilde{q}} = 1$ TeV; for [116] we take their coupling parameter
 571 $\Lambda = 1$.

572 In models of warped extra dimensions, top FCNC arise when Standard Model fermions propagate in the extra
 573 dimension with profiles governed by the corresponding Yukawa couplings. These non-trivial profiles lead to
 574 flavor-violating couplings between SM fermions and the Kaluza-Klein (KK) excitations of the SM gauge
 575 bosons. Such couplings are largest for the top quark, whose profile typically has the most significant overlap
 576 with the gauge KK modes, and lead to flavor-violating couplings that depend on 5D Yukawa couplings and
 577 the mass scale of the gauge KK modes. Appreciable flavor-violating couplings involving the top quark and
 578 Higgs boson arise from analogous processes involving loops of fermion KK modes.

579 **A possible “Discovery story”:** it is conceivable that the sensitivity of the LHC and the ILC/CLIC top
 580 FCNC could lead to the discovery and identification of physics beyond the Standard Model. An intriguing
 581 scenario is the observation of the flavor-violating decay $t \rightarrow Zc$ at the LHC with a branching ratio on the
 582 order of 10^{-5} , at the limit of the projected high-luminosity reach. Such a branching ratio would be some
 583 nine orders of magnitude larger than the Standard Model expectation and a clear indication of new physics.
 584 At the LHC the primary backgrounds to this channel are Standard Model diboson ZZ and WZ production
 585 with additional jets, with a lesser component from Z +jets and rarer SM top processes ttW and ttZ . The
 586 diboson backgrounds are fairly well understood and are in excellent agreement with simulations, and even
 587 such rare contributions as ttW and ttZ will be well-characterized by the end of the high-luminosity LHC
 588 run, making the observation of $t \rightarrow Zc$ fairly reliable.

589 A $t \rightarrow Zc$ signal described above is consistent with new physics arising from a variety of models, such
 590 as warped extra dimensions, a composite Higgs, or a flavor-violating two-Higgs-doublet model. Ancillary
 591 probes of FCNC processes become crucial for validating the signal and identifying its origin. Some of the
 592 most important probes that allow differentiation between these options are the rare decays $t \rightarrow gc$, $t \rightarrow \gamma c$,
 593 and $t \rightarrow hc$, which have similar reach at the high-luminosity LHC. In the case of warped extra dimensions
 594 or a composite Higgs, the corresponding branching ratios for $t \rightarrow gc$ and $t \rightarrow \gamma c$ are orders of magnitude
 595 below the sensitivity of the LHC, but the branching $t \rightarrow hc$ may be as large as 10^{-4} , within the reach of
 596 high-luminosity LHC. Thus a signal in $t \rightarrow Zc$ with a tentative signal in $t \rightarrow hc$ but no other channels would
 597 be indicative of warped extra dimensions or a pseudo-Goldstone composite Higgs. Such rates would also
 598 suggest a relatively low KK scale, so that complementary direct searches for heavy resonances would play
 599 a crucial role in testing the consistency of this possibility. In contrast, in flavor-violating two-Higgs-doublet
 600 models, a visible $t \rightarrow Zc$ signal can be accompanied by comparable signals in $t \rightarrow gc$ and $t \rightarrow hc$, allowing
 601 this scenario to be similarly differentiated.

602 Complementary information can be provided by the ILC. Projections of the $\sqrt{s} = 500$ GeV ILC with 500
 603 fb^{-1} place its sensitivity to $t \rightarrow Zq$ coming from a γ^μ spin structure at the level of 10^{-4} , but sensitivity to
 604 $t \rightarrow Zq$ in single top production from a $\sigma^{\mu\nu}$ structure at $\sim 10^{-5}$. The observation of comparable $t \rightarrow Zc$
 605 signals at the LHC and ILC could then favor a $\sigma^{\mu\nu}$ coupling and rule out candidate explanations such as
 606 warped extra dimensions.

607 1.5.3 Current Limits

608 Limits on various top FCNC decays have progressed rapidly in the LHC era. We summarize the current best
 609 limits from direct searches in Table 1-8. CMS places the strongest limit on the decay $t \rightarrow Zq$ in the trilepton
 610 final state [123] using the full 8 TeV data set. ATLAS sets a sub-leading limit on $t \rightarrow Zq$ using a portion
 611 of the 7 TeV data set, but also sets the leading limits on $t \rightarrow gq$ via a search for s -channel top production
 612 [124] using 7 TeV data. The Tevatron still maintains best limits on some rare processes, in particular $t \rightarrow \gamma c$

Table 1-8. Current direct limits on top FCNC. (*) denotes unofficial limits obtained from public results. The q in the final state denotes sum over $q = u, c$.

Process	Br Limit	Search	Dataset	Reference
$t \rightarrow Zq$	7×10^{-4}	CMS $t\bar{t} \rightarrow Wb + Zq \rightarrow \ell\nu b + \ell\ell q$	19.5 fb ⁻¹ , 8 TeV	[123]
$t \rightarrow Zq$	7.3×10^{-3}	ATLAS $t\bar{t} \rightarrow Wb + Zq \rightarrow \ell\nu b + \ell\ell q$	2.1 fb ⁻¹ , 7 TeV	[129]
$t \rightarrow gu$	5.7×10^{-5}	ATLAS $qg \rightarrow t \rightarrow Wb$	2.05 fb ⁻¹ , 7 TeV	[124]
$t \rightarrow gc$	2.7×10^{-4}	ATLAS $qg \rightarrow t \rightarrow Wb$	2.05 fb ⁻¹ , 7 TeV	[124]
$t \rightarrow \gamma u$	6.4×10^{-3}	ZEUS $e^\pm p \rightarrow (t \text{ or } \bar{t}) + X$	474 pb ⁻¹ , 300 GeV	[127]
$t \rightarrow \gamma q$	3.2×10^{-2}	CDF $t\bar{t} \rightarrow Wb + \gamma q$	110 pb ⁻¹ , 1.8 TeV	[125]
$t \rightarrow hq$	2.7×10^{-2}	CMS* $t\bar{t} \rightarrow Wb + hq \rightarrow \ell\nu b + \ell\ell qX$	5 fb ⁻¹ , 7 TeV	[128]
$t \rightarrow \text{invis.}$	9×10^{-2}	CDF $t\bar{t} \rightarrow Wb$	1.9 fb ⁻¹ , 1.96 TeV	[126]

613 from Run I [125] and $t \rightarrow$ invisible from Run II at CDF [126]. ZEUS maintains the best inferred limit on
 614 $t \rightarrow \gamma u$ [127]. The Tevatron and HERA limits on $t \rightarrow \gamma q$ are expected to be superseded by LHC limits using
 615 the 7+8 TeV data set, but to date no official results are available.

616 The recent discovery of the Higgs allows for limits to be set on $t \rightarrow hq$. Neither collaboration has yet placed
 617 an official limit on this process, but in [128] a limit was obtained on $t \rightarrow hq$ using the 7 TeV CMS multilepton
 618 search with 5 fb⁻¹ of data, assuming Standard Model branching ratios for a Higgs boson with $m_h = 125$
 619 GeV. Similar limits may be set using the CMS same-sign dilepton search. The CMS multilepton search has
 620 recently been updated to 5 ⊕ 9 fb⁻¹ of 7 ⊕ 8 TeV data, and now includes b -tagged categories; this should
 621 substantially increase sensitivity to $t \rightarrow hq$ in the existing data set. While multilepton final states were used
 622 to set an initial bound, limits on $t \rightarrow hq$ from the $\gamma\gamma q$ final state are likely to be about five times better
 623 than comparable multilepton limits.

624 Indirect limits on top FCNC may also be set through single top production, D^0 oscillations, and neutron
 625 EDM limits. At present these limits are not competitive with direct searches at the LHC for final states
 626 involving photons and Z bosons [130], though they are comparable for final states involving h [131].

627 1.5.4 Projected Limits

628 Although current direct limits on flavor-violating top couplings do not appreciably encroach on the parameter
 629 space of motivated theories (compare tables 1-7 and 1-8), future colliders should attain meaningful sensitivity
 630 as we now discuss (see table 1-9). Here we will focus on the sensitivity of the $\sqrt{s} = 14$ TeV LHC after 300
 631 and 3000 fb⁻¹ of integrated luminosity, as well as the ILC operating at $\sqrt{s} = 250$ and the ILC/CLIC at 500
 632 GeV, with 500 fb⁻¹ of integrated luminosity. The case of the $\sqrt{s} = 250$ GeV ILC is particularly interesting,
 633 since it possesses sensitivity to top FCNC through single-top production via a photon or Z boson.

634 1.5.4.1 LHC projections

635 At present, estimates of future LHC sensitivity to top FCNC arise from three sources: official projections
 636 from the European Strategy Group (ESG) report [132]; approximate extrapolation from current searches at

Table 1-9. Projected limits on top FCNC at the LHC and ILC. “Extrap.” denotes estimates based on extrapolation as described in the text. For the ILC/CLIC, limits for various tensor couplings are shown in (...).

Process	Br Limit	Search	Dataset	Reference
$t \rightarrow Zq$	2.2×10^{-4}	ATLAS $t\bar{t} \rightarrow Wb + Zq \rightarrow \ell\nu b + \ell\ell q$	300 fb ⁻¹ , 14 TeV	[132]
$t \rightarrow Zq$	7×10^{-5}	ATLAS $t\bar{t} \rightarrow Wb + Zq \rightarrow \ell\nu b + \ell\ell q$	3000 fb ⁻¹ , 14 TeV	[132]
$t \rightarrow Zq$	$5(2) \times 10^{-4}$	ILC single top, $\gamma_\mu (\sigma_{\mu\nu})$	500 fb ⁻¹ , 250 GeV	Extrap.
$t \rightarrow Zq$	$1.5(1.1) \times 10^{-4(-5)}$	ILC single top, $\gamma_\mu (\sigma_{\mu\nu})$	500 fb ⁻¹ , 500 GeV	[133]
$t \rightarrow Zq$	$1.6(1.7) \times 10^{-3}$	ILC $t\bar{t}$, $\gamma_\mu (\sigma_{\mu\nu})$	500 fb ⁻¹ , 500 GeV	[133]
$t \rightarrow \gamma q$	8×10^{-5}	ATLAS $t\bar{t} \rightarrow Wb + \gamma q$	300 fb ⁻¹ , 14 TeV	[132]
$t \rightarrow \gamma q$	2.5×10^{-5}	ATLAS $t\bar{t} \rightarrow Wb + \gamma q$	3000 fb ⁻¹ , 14 TeV	[132]
$t \rightarrow \gamma q$	6×10^{-5}	ILC single top	500 fb ⁻¹ , 250 GeV	Extrap.
$t \rightarrow \gamma q$	6.4×10^{-6}	ILC single top	500 fb ⁻¹ , 500 GeV	[133]
$t \rightarrow \gamma q$	1.0×10^{-4}	ILC $t\bar{t}$	500 fb ⁻¹ , 500 GeV	[133]
$t \rightarrow gu$	4×10^{-6}	ATLAS $qg \rightarrow t \rightarrow Wb$	300 fb ⁻¹ , 14 TeV	Extrap.
$t \rightarrow gu$	1×10^{-6}	ATLAS $qg \rightarrow t \rightarrow Wb$	3000 fb ⁻¹ , 14 TeV	Extrap.
$t \rightarrow gc$	1×10^{-5}	ATLAS $qg \rightarrow t \rightarrow Wb$	300 fb ⁻¹ , 14 TeV	Extrap.
$t \rightarrow gc$	4×10^{-6}	ATLAS $qg \rightarrow t \rightarrow Wb$	3000 fb ⁻¹ , 14 TeV	Extrap.
$t \rightarrow hq$	2×10^{-3}	LHC $t\bar{t} \rightarrow Wb + hq \rightarrow \ell\nu b + \ell\ell qX$	300 fb ⁻¹ , 14 TeV	Extrap.
$t \rightarrow hq$	5×10^{-4}	LHC $t\bar{t} \rightarrow Wb + hq \rightarrow \ell\nu b + \ell\ell qX$	3000 fb ⁻¹ , 14 TeV	Extrap.
$t \rightarrow hq$	5×10^{-4}	LHC $t\bar{t} \rightarrow Wb + hq \rightarrow \ell\nu b + \gamma\gamma q$	300 fb ⁻¹ , 14 TeV	Extrap.
$t \rightarrow hq$	2×10^{-4}	LHC $t\bar{t} \rightarrow Wb + hq \rightarrow \ell\nu b + \gamma\gamma q$	3000 fb ⁻¹ , 14 TeV	Extrap.

637 the 7 and 8 TeV LHC based on changes in luminosity, energy, and trigger thresholds; and dedicated study
 638 for the Snowmass process. Table 1-9 provides a summary of the projected limits at the 14 TeV LHC with
 639 300 and 3000 fb⁻¹ integrated luminosity.

640 The ATLAS projections for $t \rightarrow qZ, \gamma$ are as shown in the table. At present there is no public document
 641 from CMS with projections for 14 TeV sensitivity, nor are there official projections from either collaboration
 642 for $t \rightarrow gq$ or $t \rightarrow hq$.

643 Estimates for LHC sensitivity to $t \rightarrow gq$ and $t \rightarrow hq$ are obtained by an approximate extrapolation from
 644 current searches accounting for changes in luminosity, energy, and trigger thresholds. While crude, when
 645 applied to $t \rightarrow Zq$ this procedure agrees to within $\mathcal{O}(10\%)$ with the official ATLAS ESG projections and
 646 so provides a useful benchmark in lieu of detailed study. Applied to [128] by scaling with the luminosity
 647 and $t\bar{t}$ production cross section, this implies a 95% CL limit $\text{Br}(t \rightarrow hq) < 2 \times 10^{-3}(5 \times 10^{-4})$ with 300
 648 (3000) fb⁻¹ at 14 TeV in the multilepton final state. Similarly applied to estimates [134] of sensitivity in
 649 the $\ell\nu b + \gamma\gamma q$ final state, this suggests a 95% CL limit $\text{Br}(t \rightarrow hq) < 5 \times 10^{-4}(2 \times 10^{-4})$ with 300 (3000)
 650 fb⁻¹ at 14 TeV. The extrapolation of $t \rightarrow gq$ is more delicate, since the process under study involves the
 651 tgq anomalous coupling in the production mode. Using the results from [135] to extrapolate the observed
 652 7 TeV limit to 14 TeV, we find $\text{Br}(t \rightarrow gu) < 4 \times 10^{-6}(1 \times 10^{-6})$ with 300 (3000) fb⁻¹ at 14 TeV and
 653 $\text{Br}(t \rightarrow gc) < 1 \times 10^{-5}(4 \times 10^{-6})$ with 300 (3000) fb⁻¹ at 14 TeV.

654 1.5.4.2 Linear collider (ILC/CLIC) projections

655 At the ILC/CLIC, sensitivity studies have focused on operation at $\sqrt{s} \geq 500$ GeV in order to probe both
 656 $e^+e^- \rightarrow t\bar{t}$, $t \rightarrow Xq$ as well as the single top process $e^+e^- \rightarrow tq$ due to, e.g., tZq or $t\gamma q$ anomalous vertices⁵.
 657 Linear collider performance at $\sqrt{s} \geq 500$ GeV is studied in some detail in [133], which forms the basis
 658 for sensitivity estimates quoted here. The study [133] includes 95% CL estimates for various polarization
 659 options, including 80% e^- polarization and 45% e^+ polarization, which is close to the polarization parameters
 660 advocated for the ILC. In what follows we quote the 80%/45% polarization sensitivity, with the difference
 661 between 45% e^+ polarization and 30% e^+ polarization expected to lead to a small effect. We rescale the results
 662 of [133] to 500 fb^{-1} to match the anticipated ILC/CLIC integrated luminosity; the results are presented in
 663 Table 1-9. Based on these estimates, ILC/CLIC sensitivity at $\sqrt{s} = 500$ GeV should be comparable to
 664 LHC sensitivity with 3 ab^{-1} for $t \rightarrow Zq$ and $t \rightarrow \gamma q$. Since much of the sensitivity comes from single top
 665 production, the ILC/CLIC is less likely to provide comparable sensitivity to $t \rightarrow hq$ and $t \rightarrow gq$.

666 The ILC also provides sensitivity to tZq and $t\gamma q$ anomalous couplings at $\sqrt{s} = 250$ GeV through single top
 667 production via the s -channel exchange of a photon or Z boson, $e^+e^- \rightarrow t\bar{c} + \bar{t}c$. In fact, production via Z
 668 exchange through the γ_μ vertex reaches its maximal cross section around 250 GeV and falls with increasing
 669 center-of-mass energy. Single top production cross sections through γ exchange or Z exchange with the
 670 $\sigma_{\mu\nu}$ coupling grow with increasing energy but are still appreciable at $\sqrt{s} = 250$ GeV. The disadvantage
 671 of $\sqrt{s} = 250$ GeV relative to higher center-of-mass energies is primarily the larger SM backgrounds to the
 672 single-top final state. *In any event, this provides an intriguing opportunity for the ILC to probe new physics*
 673 *in the top sector even when operating below the $t\bar{t}$ threshold.*

674 The prospects for constraining tZq and $t\gamma q$ anomalous couplings at $\sqrt{s} = 250$ GeV have not been extensively
 675 studied, but we may extrapolate sensitivity reasonably well based on the results of [136]. To obtain an
 676 estimate, we rescale the signal cross section after cuts for $e^+e^- \rightarrow t\bar{c} + \bar{t}c$ via anomalous couplings at
 677 $\sqrt{s} = 192$ GeV in [136] to $\sqrt{s} = 250$ GeV and conservatively assume the background cross sections are
 678 similar between $\sqrt{s} = 192$ GeV and $\sqrt{s} = 250$ GeV; in actuality the backgrounds should decrease with
 679 increasing center-of-mass energy. We assume a 60% b -tag efficiency and arrive at 95% CL estimates in
 680 Table 1-9.

681 1.5.5 V_{ts} and V_{td}

682 The measurement of the ratio of top decays with b -tagging over all top decays is sensitive to the off-diagonal
 683 CKM matrix elements V_{ts} and V_{td} [137]. A measurement of this ratio at the sub-percent level should be
 684 possible at the high-luminosity LHC. The rapidity of the top quark in t -channel single top quark production
 685 is also sensitive to V_{ts} and V_{td} [138]. The ultimate precision in V_{ts} and V_{td} will come from a combination of
 686 the ratio results with their role in the different single top production modes [46]. Systematic uncertainties
 687 and their correlations between different measurements will be a limiting factor, but a precision of better than
 688 0.05 in $|V_{ts}|$ and $|V_{td}|$ should be achievable based on current studies.

⁵As mentioned in section 1.3, TLEP has larger $t\bar{t}$ samples, but no polarization so that separating couplings to γ from those to Z will be difficult.

1.5.6 Summary

Various well-motivated models predict branching ratios for top FCNC decays starting at $\sim 10^{-4} - 10^{-5}$, with the most promising signals arising in two-Higgs-doublet models and various theories with warped extra dimensions. At present the LHC sensitivity to top FCNC decays is somewhat below the level predicted by motivated theories, with the notable exception of $t \rightarrow gu$ where searches for resonant single top production yield a limit $\mathcal{O}(10^{-4})$. However, future colliders, such as the 14 TeV LHC and $\sqrt{s} = 250$ ILC or 500 ILC/CLIC, provide meaningful sensitivity to flavor-violating couplings of the top quark, of the same order as the largest rates predicted in motivated theories. The LHC and the ILC/CLIC can be complementary in this regard: while the sensitivities in tqZ/γ are (roughly) comparable for the two colliders, the LHC is better for gluon couplings, but the ILC/CLIC is the way to go for probing the spin-structure of couplings. Intriguingly, even at $\sqrt{s} = 250$ GeV the ILC should provide sensitivity to $t \rightarrow Zq, \gamma q$ that is comparable to that of the high-luminosity LHC. Finally, going to HL-LHC can improve reach by roughly a factor of two (in rates).

1.6 Probing physics beyond the Standard Model with top quarks

The top quark provides a sensitive probe for physics beyond the Standard Model, based on the following argument. The presence of new physics at the TeV scale is very well-motivated by its role in solving the Planck-weak hierarchy problem of the SM. Namely, such new particles (NP) can prevent quantum corrections from dragging the Higgs boson mass (and hence its vev, i.e., the weak scale) all the way up to Planck scale. Such NP must then necessarily couple to the Higgs boson. However, because the top quark has the largest coupling (among SM particles) to the Higgs boson, quantum corrections due to the top quark are the dominant source of destabilization of the weak scale. Thus, such NP typically also couple preferentially to the top quark (among the other SM particles).

In this section, we focus on the *direct* production of such NP, followed by their decay into top-like final states. In fact, in most solutions to the Planck-weak problem, there are actually charge $+2/3$, colored NP which accomplish this job of canceling the divergence from top quark loop in the Higgs mass (and thus stabilizing the weak scale). These can be scalar/spin-0, i.e., stops in supersymmetry (SUSY: see review in [139]). The other option being that they are fermionic (often denoted by “top-partners”), as realized in little Higgs (see reviews in [140, 141]) and composite Higgs models (the latter are conjectured to be dual to the framework of a warped extra dimension, following the AdS/CFT correspondence: see reviews in [142, 143]). The latter case is often accompanied by bosonic $t\bar{t}$ resonances. With the above motivation, the studies performed for Snowmass process can be grouped into the following three categories: searches for stops, top-partners and $t\bar{t}$ resonances and these are described in turn below.

Note that virtual/indirect effects of such NP also lead to rare/neutral current decays of the top quark which are discussed in section 1.5 of this report. In addition, there can be shifts in already-existing-in-the SM (for example, flavor-preserving) couplings of the top quark, as discussed in section 1.3 of this report. Finally, these studies have overlap with work of the Snowmass Beyond Standard Model group [144].

1.6.1 Stops

SUSY is perhaps the most popular solution to the Planck-weak hierarchy problem of the SM. It involves addition of a *superpartner* for every particle of the SM, with a spin differing by 1/2-unit from that of the corresponding SM particle. While in general superpartner masses in SUSY models are very model-dependent, naturalness strongly suggests that the scalar partners of the top quark, or *stops*, should have masses around the weak scale. The reason is that (as mentioned above) the stops cancel the largest divergence in the Higgs mass squared parameter, namely that from SM top loop. This makes stops a prime target for LHC searches. The results of such searches are typically presented in terms of the “vanilla stop” simplified model, which contains two particles, a stop \tilde{t} and a neutralino LSP $\tilde{\chi}^0$ (i.e., superpartner of photon and Z or Higgs boson). The stop is assumed to decay via $\tilde{t} \rightarrow t\tilde{\chi}^0$ with a 100% branching ratio. Within this model, the current “generic” bound on the stop mass is about 700 GeV [145, 146]. One of the tasks of future experiments is obviously to improve the reach on $m(\tilde{t})$ for generic spectra. In fact, both ATLAS and CMS have presented estimates of the discovery reach of LHC-14 and HL-LHC in the vanilla stop model, extrapolating the present 1-lepton search [147, 148]. For a “generic” spectrum, stops up to approximately 800 (900) GeV can be discovered, at a 5- σ level, with 300 fb $^{-1}$ (3 ab $^{-1}$) integrated luminosity. It is interesting to determine if the reach at LHC 14 TeV for this generic case can be extended beyond the above ATLAS/CMS projections using *special* techniques developed recently and so far applied only to the LHC 7/8 TeV. The first study (as part of the Snowmass process) mentioned below is along these lines.

Moreover, it must be emphasized that lighter stops are still allowed by LHC 7/8 TeV. In particular:

- (a) If $m(\tilde{\chi}^0) > 250$ GeV, stops of any mass are allowed;
- (b) in the “off-shell top” region, $m_t > m(\tilde{t}) - m(\tilde{\chi}^0) > m_W$, stops above 300 GeV are allowed;
- (c) in the “compressed” region, $m(\tilde{t}) \approx m(\tilde{\chi}^0) + m_t$, stops of any mass are allowed (this includes the particularly challenging “stealthy” region, $m(\tilde{t}) \approx m(t) \gg m(\tilde{\chi}^0)$); and
- (d) in the “squeezed” region, $m(\tilde{t}) - m(\tilde{\chi}^0) < m_W$, stops of any mass are allowed.

In all these regions, kinematics of stop production and decay yields events with little missing transverse energy (MET), reducing the efficiency of LHC searches. Thus, another goal of future experiments should be to explore the special regions listed above. A couple of studies to cover the stealth stops of case (c) above were done as part of Snowmass process and are outlined below.

Although LHC will clearly play a leading role in the generic case⁶, it should be emphasized that in any of the special regions, stops can still be within the kinematic reach of the ILC/CLIC, at $\sqrt{s} = 500$ GeV or 1 TeV. In this case, the ILC could play a crucial role in discovering the stops and precisely determining/confirming their properties, *e.g.* spin and masses.

Finally, *addition* of particles (such as gluino or chargino, i.e., superpartners of SM gluon or W) to the above simplified model is well-motivated. Studies along these lines were also performed for the Snowmass process and are described below.

⁶direct production of stops at the ILC in this region is not possible, given the current bounds

Collider	Energy	Luminosity	Cross Section	Mass
LHC8	8 TeV	20.5 fb ⁻¹	10 fb	650 GeV
LHC	14 TeV	300 fb ⁻¹	4.6 fb	990 GeV
HL LHC	14 TeV	3 ab ⁻¹	1.4 fb	1.2 TeV

Table 1-10. The first line gives the current bound on stops. The remaining lines give the estimated reach in stop pair production cross section and mass for different future hadron collider runs.

Collider	Luminosity	Technique	Reach
LHC 14 TeV	100 fb ⁻¹	spin-correlations	200 GeV (5 σ)
LHC 14 TeV	100 fb ⁻¹	dileptonic m_{T2}	185–195 GeV (5 σ)
LHC 14 TeV	300 fb ⁻¹	VBF	233 GeV (3 σ)

Table 1-11. Reach for stealth stops.

1.6.1.1 Vanilla stops

Here fully hadronic decays using strategies inspired by [149, 150, 151, 152] are considered. The fully hadronic channel has two advantages over leptonic searches. The first is that it has the largest branching fraction for the top decays. The second is that it has no inherent missing energy from neutrinos, so all the missing energy comes from the neutralinos. This allows many backgrounds to be reduced by vetoing events with leptons. Jet-substructure based top tagging (see section 1.7 of this report) is used to distinguish signal from background. The results are summarized in table 1-10: for more details, see reference [153].

1.6.1.2 Stealth stops

In the above-mentioned ATLAS/CMS projections of reach for stops at LHC 14 TeV, significant gaps in the coverage remain: for example, no discovery is possible for the LSP mass above 500 GeV, as well as in the compressed and stealthy regions, even at HL-LHC. It is clear that novel search strategies will be needed to cover these regions.

Two studies of such strategies were contributed to our working group (see table 1-11 for summary of results). Reference [154] focused on the stealthy stop region, which is particularly challenging since, unlike the region with a heavy neutralino, no significant MET is generated even in the presence of ISR jets. The challenge is to distinguish $\tilde{t}\tilde{t}^*$ events from a much larger $t\bar{t}$ background. Two methods to achieve this task have been studied: (a) using spin correlations, which are present in $t\bar{t}$ but not in $\tilde{t}\tilde{t}^*$ events, due to \tilde{t} being a scalar particle [80] (see also section 1.4.2 of this report); and (b) using an m_{T2} cut in dileptonic event sample [155]. It was found that, using spin correlations, LHC-14 with 100 fb⁻¹ of data will be able to discover the stealthy stop at the 5 σ level, assuming the stop mass of 200 GeV. Assuming a 15% systematic error, the m_{T2} method will be able to discover right-handed stops in the (185, 195) GeV window, while the sensitivity to the left-handed stop is poor due to the absence of a long m_{T2} tail in the signal in this case.

The second study [156] analyzed the possibility of using the vector boson fusion stop production channel, which provides additional jets that could be used to tag the events with stealthy, compressed, or light stops. It was found that, for example, the LHC-14 with 300 fb⁻¹ of data will be able to probe the scenario with $m(\tilde{t}) = 233$ GeV and $m(\tilde{\chi}^0) = m(\tilde{t}) - m_t$, at a 3 σ level.

Collider	Luminosity	Reach
LHC 14 TeV	10 fb ⁻¹	1.4 TeV
LHC 14 TeV	300 fb ⁻¹	? TeV
LHC 14 TeV	3000 fb ⁻¹	? TeV

Table 1-12. Reach for gluino decaying into stops, with R -parity conservation

Collider	Luminosity	Technique/channel	Reach
LHC 14 TeV	300 fb ⁻¹	topness, asymmetric	800 GeV
LHC 14 TeV	3000 fb ⁻¹	topness, asymmetric	1.2 TeV
LHC 14 TeV	? fb ⁻¹	dilepton, well-tempered neutralino	? GeV

Table 1-13. Reach for stops decaying into chargino.

1.6.1.3 Gluino-initiated stop production

In addition to stops, naturalness also strongly motivates a light gluino, constraining its mass through the one-loop QCD correction to stop mass. A rough naturalness bound is $m(\tilde{g}) < 2m(\tilde{t})$ [157]. This motivates considering a simplified model with gluino, stop and an LSP, with a decay $\tilde{g} \rightarrow t\bar{t} + \text{MET}$. Assuming that this decay proceeds via an off-shell stop and has a 100% branching ratio, LHC-8 searches rule out gluino masses up to about 1.3 TeV, provided that the LSP mass is below 500 GeV [158, 159]. Extrapolating the search in the all-hadronic channel, CMS estimates a 5σ discovery reach of 1.7 TeV at LHC-14 with 300 fb⁻¹ of data [148]. For gluino masses above TeV, “boosted” (relativistic in the lab frame) tops become increasingly common in \tilde{g} decays. In this regime, boosted top tagging techniques (see section 1.7 of this report), developed and tested at the LHC for non-SUSY applications, can be used to provide a novel handle to search for SUSY. A preliminary study (with no detector simulation) suggests that gluinos with masses up to 1.4 TeV can be discovered at the LHC-14 with only 10 fb⁻¹ of data, using top-tags in combination with more traditional cuts in all-hadronic events [160].

1.6.1.4 Including more electroweak particles

Another well-motivated extension of the vanilla stop simplified model is to add a chargino $\tilde{\chi}^\pm$, with $m(\tilde{\chi}^\pm) < m(\tilde{t})$. This is also motivated by naturalness, since the charged Higgsino mass is controlled by the μ parameter which cannot be far above 100 GeV in natural SUSY models [157]. This simplified model has the possibility of *asymmetric* stop events: *e.g.* $pp \rightarrow t\bar{t}^*$, $\tilde{t} \rightarrow t\tilde{\chi}^0$, $\tilde{t}^* \rightarrow b\tilde{\chi}^\pm$. A study of the LHC sensitivity to this signal was performed: for details, see reference [161]. The proposed search uses the 1-lepton+MET channel, and relies crucially on the “topness” variable, introduced in [162] as a general tool to suppress the $t\bar{t}$ background in this channel. It was found that 5σ discovery is possible at LHC-14 with 300 fb⁻¹ for stop masses up to about 800 GeV, if $m(\tilde{\chi}^0)$ is below about 300 GeV. With 3000 fb⁻¹, the discovery reach extends to stop masses about 1.2 TeV for light $\tilde{\chi}^0$.

A related simplified model was used in the study in reference [163]. Motivated by the “well-tempered neutralino” dark matter scenario [164], this study considered a spectrum with light bino and Higgsino, leading to three neutralino and one chargino states at the bottom of the SUSY spectrum (it was assumed that all these states are lighter than the stop). The analysis focused on the dilepton signature, where the leptons can come either from top decays or from $\chi_{2,3}^0 \rightarrow Z\chi_1^0$. It was found that the reach is XXX TeV.

Collider	Luminosity	Technique	Reach
LHC 14 TeV	100 fb ⁻¹	same-sign dilepton	1.3–1.4 TeV
LHC 14 TeV	? fb ⁻¹	single-lepton, reconstruct mass	? TeV

Table 1-14. Reach for gluino decaying into stops, with R -parity violation.

1.6.1.5 R -parity violation

Yet another interesting scenario is R -parity violating (RPV) supersymmetry, where decay modes are modified relative to the above cases of R -parity conservation. For example, a stop can decay via $\tilde{t} \rightarrow \bar{b}\bar{s}$ induced by the UDD superpotential operator. This scenario emerges naturally from models with minimal flavor violation [165, 166]. Direct stop production in this case yields all-hadronic final states, but it might still be possible to search in this channel: see, for example, the Snowmass study [167]. However, just as in conventional SUSY, naturalness strongly suggests the presence of relatively light gluinos. Gluino decays via cascades involving stops, $\tilde{g} \rightarrow \tilde{t}t, \tilde{t} \rightarrow 2j$, may be observable, even though they do not produce large MET. If \tilde{g} is Majorana, as in simplest SUSY models, such decays can provide a striking same-sign dilepton (SSDL) signature. Current SSDL searches already rule out gluinos up to 800 GeV, independent of the stop mass, in the RPV scenario [168]. At LHC-14 with 100 fb⁻¹ of data, the projected reach of this search is 1.3 – 1.4 TeV, again approximately independent of the stop mass [168]. This estimate includes an improvement in sensitivity due to an additional requirement of one or two massive jets. (The massive jets can be either due to boosted stop decays, or to accidental mergers of neighboring jets in a high jet multiplicity signal event.) An alternative is a search in a single-lepton channel, which has a higher rate and applies to both Majorana and Dirac gluinos [169]. In this case, the requirement of stop mass reconstruction from jet pairs can be used as an additional handle to suppress backgrounds. At the 14 TeV LHC, this search will be sensitive to gluino masses up to XXX TeV [170].

1.6.2 Top-partners

As mentioned above, in alternative solutions to the Planck-weak hierarchy problem, the divergence in Higgs mass squared parameter from SM top loop is canceled by new *fermions* which are vector-like under the SM gauge symmetries, in particular, they are color triplets with electric charge 2/3 (i.e., same as the SM top and hence these new particles are dubbed top-partners. Such particles can also arise in other extensions of the SM so that it is useful to follow a model-independent, simplified approach in studying their signals. The top-partners can be produced via QCD interactions in pairs or singly [171], the latter resulting from coupling of top-partner to SM top/bottom, as needed to cancel the SM top divergence in Higgs mass squared parameter.

Based on the $SU(2)_L$ gauge symmetry of the SM, the top-partners are often accompanied by “bottom-partners”. Finally, in some composite Higgs models, an extension of the EW symmetry group (from that in the SM) is motivated by the goal of avoiding constraints from $Zb\bar{b}$ [172]: this results in the appearance of color triplet, but charge 5/3 particles (in addition to the above top/bottom partners).

In short, there are three types of vector-like quarks which are well-motivated extensions of the SM, namely, top and bottom-partners and charge-5/3 fermions. Once produced, these vector-like quarks can decay into a top-like final state. All these cases were studied for various LHC scenarios as part of the Snowmass process (including both single and pair production of top-partners mentioned above) and are discussed below. Note

Collider	Luminosity	Pileup	95 % exclusion mass
LHC 14 TeV	300 fb ⁻¹	0	1.4 TeV
LHC 14 TeV	300 fb ⁻¹	50	TeV
LHC 14 TeV	3 ab ⁻¹	0	1.75 TeV
LHC 14 TeV	3 ab ⁻¹	140	? TeV
LHC 33 TeV	3 ab ⁻¹	225	? TeV

Table 1-15. *Expected sensitivity for a top-partner pair production in the lepton + jets channel.*

Collider	Luminosity	Pileup	95 % exclusion	5 σ discovery
LHC 14 TeV	300 fb ⁻¹	50	? TeV	? TeV
LHC 14 TeV	3 ab ⁻¹	140	? TeV	? TeV
LHC 33 TeV	3 ab ⁻¹	?	2.2 TeV	1.75 TeV

Table 1-16. *Expected mass sensitivity for a top-partner single production via decay into th .*

855 that given the current (LHC 7/8 TeV) bounds on these quarks of at least 500 GeV [173, 174], their direct
856 production at the ILC is not possible.

857 1.6.2.1 Pair production of top-partners

858 The top-partner has three possible decay modes: bW , tH and Zt . The interesting feature is that, in the limit
859 of a heavy top-partner, the decay modes are equally shared by these three modes (following the principle of
860 Goldstone equivalence). Reference [175] contains more details of the analysis, whose main conclusions are
861 given in table 1-15.

862 1.6.2.2 Single production of top/bottom-partners

863 As mentioned earlier, the single production proceeds by means of the top/bottom-partners electroweak
864 effective couplings to a weak boson and a SM quark, which are precisely the ones relevant for canceling top
865 quark induced divergence in Higgs mass. These production mechanisms have larger rates than those of pair
866 productions for *heavier* top/bottom partners. Moreover, analyses of single-production channels might permit
867 the measurement of the above-mentioned effective couplings. Note that the top-partner single-production,
868 that proceeds via the intermediate exchange of a bottom quark has a rate significantly higher than those of
869 single bottom partner and charge-5/3 productions, which are mediated by the exchange of a top. Hence, for
870 bottom partners and charge 5/3 quarks, only pair production is considered.

871 As mentioned above, the top-partner can decay into one of three possible final states: ht , Zt and Wb . Since
872 the W + jet backgrounds are considerable for the third mode, here the focus was on the first two decay
873 modes. The basic idea is to reconstruct the top-partner mass: for more details, see reference [176]. The
874 results are summarized in table 1-16.

Collider	Luminosity	Pileup	95 % exclusion
LHC 14 TeV	300 fb ⁻¹	50	? TeV
LHC 14 TeV	3 ab ⁻¹	140	? TeV
LHC 33 TeV	3 ab ⁻¹	50	? TeV
LHC 33 TeV	3 ab ⁻¹	140	? TeV

Table 1-17. Expected mass sensitivity for a bottom-partner pair production.

Collider	Luminosity	Pileup	3 σ evidence	5 σ discovery
LHC 14 TeV	300 fb ⁻¹	50	1.45 TeV	1.33 TeV
LHC 14 TeV	300 fb ⁻¹	140	1.43 TeV	1.32 TeV
LHC 14 TeV	3 ab ⁻¹	50	1.54 TeV	1.44 TeV
LHC 14 TeV	3 ab ⁻¹	140	1.51 TeV	1.40 TeV
LHC 33 TeV	300 fb ⁻¹	50	2.18 TeV	2.00 TeV
LHC 33 TeV	300 fb ⁻¹	140	2.17 TeV	1.96 TeV
LHC 33 TeV	3 ab ⁻¹	50	2.24 TeV	2.15 TeV
LHC 33 TeV	3 ab ⁻¹	140	2.24 TeV	2.07 TeV

Table 1-18. Expected mass sensitivity for a charge 5/3 pair single production via decay into tW^+ .

875 1.6.2.3 Pair production of bottom-partners

876 The decays of bottom-partners can be into W^-t , Zb , or Hb . Thus, pair production of bottom partners can
 877 lead to interesting signal of same-sign dileptons via $W^-tW^+\bar{t} \rightarrow b\bar{b} 2W^+ 2W^-$, followed by leptonic decays
 878 of both W^+ (or W^-). More details of this study can be found in reference [177]; here, only the final results
 879 are shown in table 1-17.

880 1.6.2.4 Pair production of Charge-5/3 fermion

881 The interesting feature [178] of charge-5/3 vector-like fermion is that decay of *single* such quark can gives
 882 rise to *same*-sign dileptons, i.e., final state is $tW^+ \rightarrow bW^+W^+$, followed by leptonic decays of both W^+ 's.
 883 The table 1-18 displays the reach for these exotic quarks; for more details, see reference [179].

884 1.6.3 $t\bar{t}$ resonances

885 As mentioned earlier, in non-supersymmetric solutions to the Planck-weak hierarchy problem, there are
 886 typically bosonic new particles which decay dominantly into $t\bar{t}$. Examples are leptophobic Z' 's in topcolor
 887 models [180] or KK gluons in warped extra dimensional frameworks (conjectured to be dual 4D composite
 888 Higgs models: see reviews in [142, 143]). Moreover, such $t\bar{t}$ resonances are favored to be rather heavy (a
 889 few TeV) due to the constraints from various precision tests. and/or by the current direct bounds from
 890 LHC 7/8 TeV [181, 182, 183, 184]. Thus, the top quarks resulting from their decays are boosted so that
 891 the top decay products can be quite collimated, requiring special identification techniques which have been

Collider	Luminosity	Pileup	95 % exclusion	5 σ discovery
LHC 14 TeV	300 fb ⁻¹	50	3.9 TeV	3.0 TeV
LHC 14 TeV	3 ab ⁻¹	140	? TeV	? TeV

Table 1-19. Expected mass sensitivity for a Z' decaying into dileptonic $t\bar{t}$.

Collider	Luminosity	Pileup	95 % exclusion for Z'	95 % exclusion for KK gluon
LHC 14 TeV	300 fb ⁻¹	50	? TeV	~ 4.5 TeV
LHC 14 TeV	3 ab ⁻¹	140	? TeV	~ 6.5 TeV

Table 1-20. Expected mass sensitivity for a Z' and KK gluon decaying into semileptonic and fully hadronic $t\bar{t}$, using jet mass/Snowmass top-tagger.

892 developed recently (for more details, see section 1.7 of this report). In some models, these $t\bar{t}$ resonances can
893 also be broad, thereby adding to the challenge of searching for them.

894 Three such studies of discovery of $t\bar{t}$ resonances were done as part of the Snowmass process and are discussed
895 in what follows. Of course, post-discovery, the focus will shift to determination of the quantum numbers
896 of these $t\bar{t}$ resonances. For example, the spin and chiral structure of couplings of these resonances can be
897 measured via angular distribution and polarization of the resulting top quarks: see, for example, references
898 [185, 186, 82]. Finally, note that given the mass range of these $t\bar{t}$ resonances, ILC/CLIC would not play a
899 role in a direct search.

900 1.6.3.1 Dileptonic

901 This study focused on W 's from both top quarks decaying into lepton (called "dileptonic" $t\bar{t}$). Obviously,
902 one expects hadronic activity near the leptons due to the boosted nature of the tops. So, SM $t\bar{t}$ background
903 can be suppressed by in fact requiring *smaller* separation between lepton and closet jet: for details, see
904 reference [187]. The results are summarized in table 1-19.

905 1.6.3.2 Semileptonic and fully hadronic

906 Alternatively, one of the two W 's from the decays of the top quarks can give a lepton, while the other one
907 decays into hadrons (semileptonic $t\bar{t}$) or none of the two W 's decays into leptons (fully hadronic $t\bar{t}$). The
908 first study of this kind utilized jet mass/Snowmass top-tagger for dealing with boosted top quarks. The
909 results are expressed in terms of both Z' and KK gluon in warped extra dimensional models: see table 1-20.

910 Another study focused on KK gluon in warped extra dimensional models. In order to identify boosted top
911 quarks, it used the Template Overlap Method (TOM) [188]. TOM has been extensively studied in the past
912 in the context of theoretical studies of boosted tops and boosted Higgs decays [189], as well as used by the
913 ATLAS collaboration for a boosted resonance search [183]. The method is designed to match the energy
914 distribution of a boosted jet to the parton-level configuration of a boosted top decay, with all kinematic
915 constraints taken into account. Low susceptibility to intermediate levels of pileup (i.e. 20 interactions per
916 bunch crossing), makes TOM particularly attractive for boosted top analyses at the LHC. For more details
917 about how the TOM is used in this study, see reference [190]: the results are shown in table 1-21.

Collider	Luminosity	Pileup	95 % exclusion
LHC 14 TeV	300 fb ⁻¹	50	? TeV
LHC 14 TeV	3 ab ⁻¹	140	? TeV
LHC 33 TeV	3 ab ⁻¹	225	? TeV

Table 1-21. Expected mass sensitivity for a KK gluon decaying into semileptonic and fully hadronic $t\bar{t}$, using the template overlap method.

918 1.6.3.3 Single-top resonance

919 Resonances can appear not only in top pair production, but also in single top quark production. This final
 920 state is particularly sensitive to a high-mass W' boson that couples primarily to quarks. Current limits for
 921 W' production are around 1.8 TeV [191, 192, 193]. A Snowmass study shows that the reach for W' can be
 922 extended to 5 TeV (6 TeV) with 300 fb⁻¹ (3000 fb⁻¹) at the 14 TeV LHC [194].

923 In warped extra dimensional models, the KK gluon discussed in the previous section can also have a sub-
 924 dominant decay into $t\bar{c}$ (and $\bar{t}c$) [195]. This process is also relevant for the flavor sector, see the chapter on
 925 Flavor working group [196]. The final state has a single top quark, just like $W' \rightarrow tb$, but now the other quark
 926 jet is from a charm quark rather than a bottom quark. This has consequences for the b -tag multiplicity and
 927 background suppression. The Snowmass study finds a mass limit on KKg of about 3.5 TeV if the branching
 928 ratio to tc is 20%. If this branching ratio is less than 5%, the signal is buried below backgrounds and no
 929 limit can be set.

930 A fourth-generation quark with chromomagnetic couplings will be visible in the single top plus W boson
 931 final state [197, 198]. Due to the strong nature of the b^* production process, the reach for this particle at
 932 the high-luminosity LHC should be multi-TeV, similar to the W' .

933 1.7 Top Algorithms and Detectors

934 Studies of top quarks at future colliders will, in many cases, require dealing with new environments. These
 935 include the increased number of pile-up events per bunch crossing in the high-luminosity phase of the LHC
 936 and an increasing reliance on boosted techniques for top identification as higher energy of the LHC and
 937 stronger constraints on scale of BSM physics will require exploration of higher invariant mass events in top
 938 quark pair production. In this Section we discuss how existing algorithm for top quark studies fare in these
 939 cases and whether or not physics studies that we described in the preceding Sections are in fact viable given
 940 difficult experimental environments of new colliders. We also discuss the unique experimental conditions of
 941 the linear collider for top quark studies.

942 1.7.1 Top quark identification at low transverse momentum

943 The majority of top quarks produced at the LHC have low transverse momenta. Measurements of the total
 944 and differential $t\bar{t}$ cross sections (Sections 1.4 and 1.3), of the top-quark mass (Section 1.2), charge asymmetry
 945 (Section 1.4), and single-top measurements (Section 1.3) all require precise and efficient reconstruction of
 946 top quarks at low transverse momenta. Top-quark reconstruction at low transverse energies is limited by

947 a number of factors that determine total systematic uncertainty, including: a) jet-energy scale uncertainty
 948 which typically accounts for 50% of the overall uncertainty in traditional top-quark measurements based
 949 on jets; b) jet-energy resolution uncertainty; c) b -tagging efficiency uncertainty and mistag rates; and d)
 950 uncertainty on missing transverse-energy reconstruction. This indicates that any further progress in precision
 951 top measurements at low p_{\perp} that involves jet reconstruction can only come from a better understanding of
 952 low- p_T jets⁷ and b -tagging.

953 The high-luminosity upgrade of the LHC will have an important impact on low- p_{\perp} top physics. Indeed, more
 954 than 100 pileup events per bunch crossing will have a negative impact on many final-state observables, but
 955 primarily on low- p_T jets and b -tagged jets due to their large associated systematics. Studies of this scenario
 956 [199] were performed for pp collisions at a center-of-mass energy of $\sqrt{s} = 14$ TeV using a fast detector
 957 simulation based on the Delphes 3.08 framework [200]. Jets are reconstructed at the LHC using the anti-
 958 k_T algorithm [201] with distance parameter $R = 0.4$ (ATLAS) and $R = 0.5$ (CMS and Snowmass-specific
 959 studies). These high-luminosity MC simulation studies showed that, in general, pileup events deposit energy
 960 in many calorimeter cells and hence shift the raw jet transverse energies by approximately 50 (120) GeV
 961 for 50 (140) pileup events, adding about one additional GeV for each pileup event. This energy needs to be
 962 subtracted jet-by-jet using average energies deposited elsewhere in the calorimeter. The use of tracking in jet
 963 reconstruction is also useful, not only in refining the jet energy measurement but also to mitigate the impact
 964 of pileup. Nevertheless, the subtraction of pileup results in smeared jet transverse momenta. In addition,
 965 there will be a flux of low- p_T fake jets created from pileup events. While tracking can be used to address
 966 some of these issues as well, pileup also creates many additional tracks that need to be separated from the
 967 tracks belonging to each jet in an event.

968 Figure 1-5(a) shows the effect of different pileup scenarios on the jet p_T distribution. One consequence
 969 of the energy shift is that for the selection of top quark signal jets, a pileup subtraction technique should
 970 correct energies of the signal jets by 200-400%, leading to larger uncertainties compared to previous analyses.
 971 Uncertainties due to pileup will become dominant, and are expected to increase by a factor of two or more
 972 at the highest LHC luminosity. As an example, a 2% jet-energy scale uncertainty for a jet measurement
 973 without pileup translates to a 3%(5%) uncertainty in case of 50 (140) pileup events scenario.

974 Since uncertainties in jet resolution, jet energy scales, and b -tagging are dominant uncertainties in many
 975 measurements related to top quarks, it is to be expected that precision of such measurements will not
 976 improve at higher luminosities and will deteriorate unless new jet energy calibration methods are adopted.
 977 Data-driven techniques may improve the assessment of the jet energy scale, but it is unlikely that this can
 978 make a significant difference to the above conclusion. As the result, the standard top mass measurements
 979 do not improve at the high-luminosity phase of the LHC, as we discuss in Section 1.2.

980 The reconstruction of the top quark mass that is used in many other top quark analyses will also be degraded
 981 by the high pileup in high-luminosity runs. A DELPHES MC study shows that using the trijet mass for top-
 982 reconstruction is strongly affected by pileup events even when particle-flow methods and pile-up subtraction
 983 techniques are used to mitigate the problem [199]. Figure 1-5(b) shows the reconstructed top mass using
 984 a procedure similar to the one discussed in [202]. It was also observed [199] that the trijet mass for top-
 985 reconstruction strongly depends on top transverse momentum p_T due to large jet multiplicity from ISR/FSR.
 986 For $p_T > 700$ GeV, the peak position is at 400 GeV, assuming the same transverse momentum cuts as for
 987 low- p_T measurements. This may limit our ability to identify top quarks at such large p_T using the traditional
 988 low-energy approaches.

989 Runs at high pileup will also affect other top physics measurements, such as $t(\bar{t})$ +jets and associated top
 990 production (such as $Ht\bar{t}$), discussed in Section 1.3, as well as searches for new physics that require a good
 991 understanding of low- p_T top quarks, for example searches for rare top decays (Section 1.5). Indeed, low- p_T

⁷By “low”- p_{\perp} we mean jets with transverse momenta in the range 25 – 50 GeV.

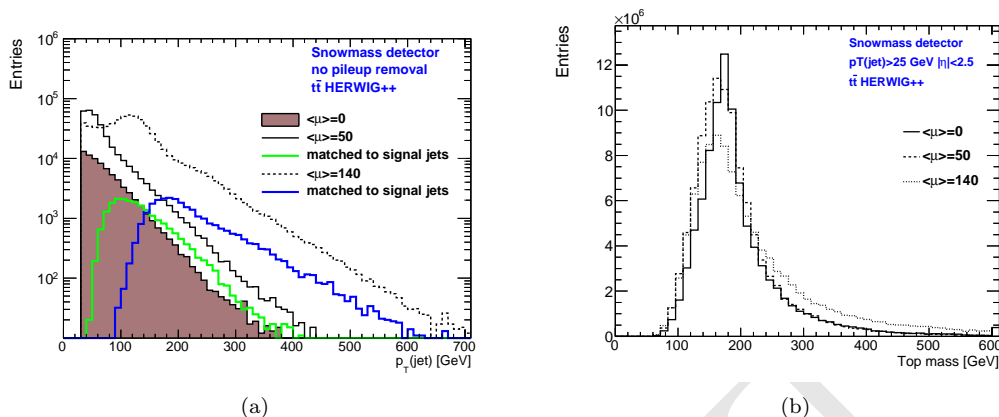


Figure 1-5. (a) Plots of jet p_T distributions for different pileup scenarios using the DELPHES simulation. Also shown are only the jets matched to the top quarks in the event for each pileup scenario, demonstrating the large effect of additional pileup events on top quark reconstruction. (b) Reconstructed top quark masses from trijets by requiring at least four jets with $p_T > 25 \text{ GeV}$ and $|\eta| < 2.5$, and at least one of the jets must be tagged by a b -tagging algorithm.

992 top quarks require the reconstruction of jets with transverse momentum 30 – 100 GeV, which are exactly
 993 the jets that are difficult to correct for pileup effects. These measurements are also affected by the reduced
 994 performance of b -tagging at high pileup.

995 Perhaps only a combination of multiple measurements by CMS and ATLAS may lead to substantial reduction
 996 of systematic detector uncertainties, as the high-luminosity pp collision runs at 14 TeV with more than
 997 hundred pile-up events are unfavorable for high precision top quark measurements based on jets with
 998 transverse momenta below 100 GeV. This will also affect searches for new physics that require detection
 999 of low- p_{\perp} jets from top decays. It is therefore important to discuss the future of boosted measurements,
 1000 where additional reconstruction techniques can be utilized.

1001 1.7.2 Boosted top quarks

1002 As we explained in Section 1.6, top quarks play a very important role in many searches for new particles
 1003 at the highest energies. We find that current algorithms for top quark identification at high- p_T can lead to
 1004 performance that is similar to what is achieved in current experiments, provided that some modifications to
 1005 the reconstruction methods are implemented or detectors upgrades are performed.

1006 The decay products of a top quark with high p_T are sufficiently collimated to be reconstructed within a
 1007 single jet. This happens above $\sim 400 \text{ GeV}$ for jets with $R = 0.8$. Figure 1-6 shows the evolution of jet mass
 1008 with the jet transverse momentum for the $t\bar{t}$ process. Because all of the top decay products fall within a
 1009 single jet, specialized techniques involving jet substructure are required [203, 204]. Semileptonic top decay
 1010 reconstructions must introduce modified isolation criteria when the lepton starts to overlap with the b quark
 1011 jet from the top decay. This reconstruction of the top mass within a single jet itself is a good discriminant
 1012 between boosted top quarks and the overwhelming background from QCD jet production. For example, a
 1013 recent study [73] has shown that a signal of boosted hadronic top quarks from a Z' boson decay can be
 1014 observed in the jet mass distribution alone for jets with $p_T > 800 \text{ GeV}$. Discrimination can possibly be

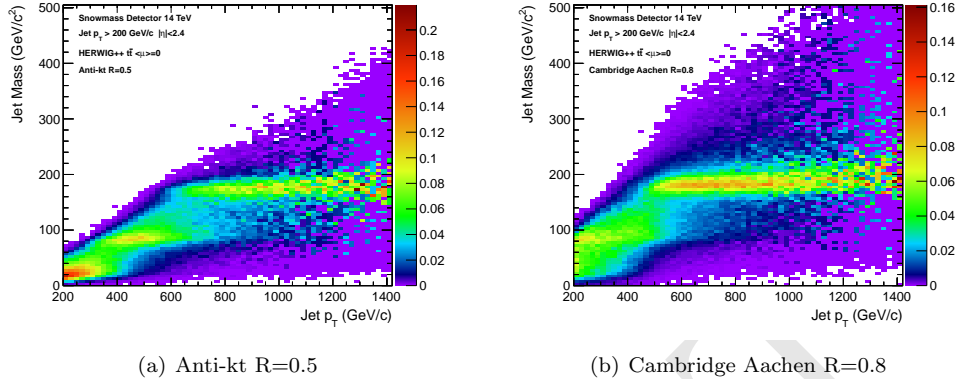


Figure 1-6. Jet mass vs jet transverse momenta in the DELPHES fast simulation for pp collisions at 14 TeV for different jet algorithms. The jet transverse spectrum has been reweighed to be flat.

1015 improved further with the addition of b -tagging. The reconstruction of the top jet through its proximity to
 1016 the mass of the top is the basic idea behind the boosted top studies. In addition, further signal/background
 1017 separation is achieved by using specialized algorithms that split the top jet into sub-jets and then manipulate
 1018 those to determine if observed jet substructure is consistent with soft and collinear QCD radiation or with
 1019 the decay of a heavy object into jets through a point-like interaction vertex.

1020 **Jet grooming.** Boosted jets are affected by pileup just like the unboosted ones discussed in Section 1.7.1.
 1021 Several algorithms, collectively known as jet grooming algorithms, attempt to mitigate the effect of pileup
 1022 on jet observables, such as jet mass, by removing soft and wide-angle constituents of jets. The effect of three
 1023 different jet grooming algorithms have been studied: pruning [205, 206], trimming [207], and filtering [208].
 1024 The application of these jet grooming algorithms results in a jet mass distribution that is relatively stable
 1025 as the number of pileup events increases. Additionally, the jet grooming procedures significantly reduce the
 1026 masses of QCD jets, enhancing signal/background discrimination significantly.

1027 **Substructure and jet shapes.** Jet substructure and jet shapes are often discussed as a useful tool for the
 1028 identification of top quarks and for reduction of the overwhelming rate from conventional QCD processes
 1029 [185, 209, 210, 211, 212, 213, 214, 215, 206, 216, 217, 188, 218, 219, 220, 221]. For example, the N -subjettiness
 1030 algorithm [222] aims to determine the consistency of a jet with a hypothesized number of subjets. Such tools
 1031 can give good discrimination between top quark jets and QCD jets, however, such discrimination degrades
 1032 somewhat with the additional pileup activity.

1033 It is also beneficial to identify the two subjets corresponding to the W boson produced in the top quark
 1034 decay. Using trimming, a W mass peak can be extracted which is relatively stable even with 140 additional
 1035 pileup events added.

1036 **Top tagging.** In addition to the substructure quantities described above, there are several algorithms (top
 1037 taggers) which combine multiple jet observables to identify top jets and provide additional discrimination
 1038 from QCD jets. Two top-tagging algorithms which are currently in use by experimental efforts include
 1039 the CMS Top Tagger [217, 213] and the HEP Top Tagger [149, 223, 224, 225, 183]. The CMS top tagger
 1040 decomposes a jet into up to 4 subjets. Then requirements on the jet mass ($140 < m_j < 250$ GeV), number
 1041 of subjets (3 or more) and a quantity which is a proxy for the mass of the W boson within the jet (minimum
 1042 pairwise subjet mass > 50 GeV), are imposed to isolate boosted top quarks. We have studied the effect

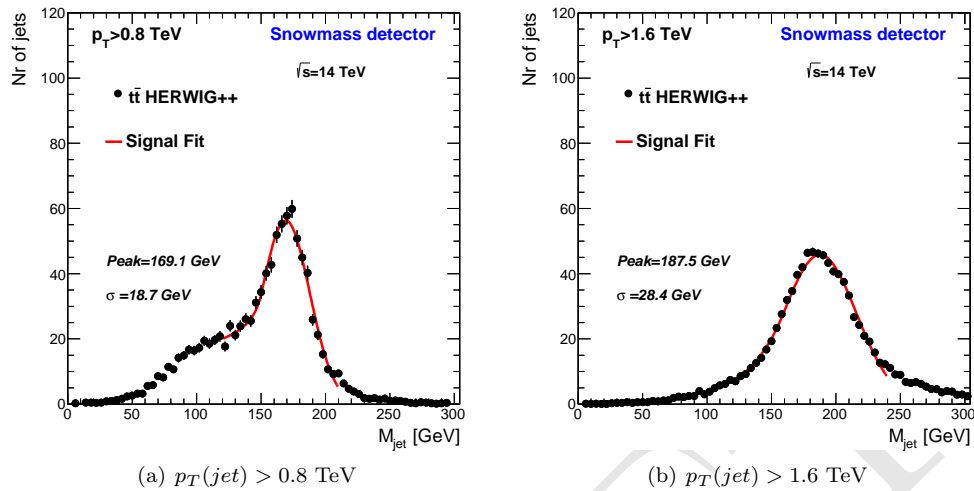


Figure 1-7. Jet mass for $t\bar{t}$ events for different $p_T(\text{jet})$ and $\langle\mu\rangle = 140$. The core of the peak was fitted using a Crystal Ball function [226]. All histograms are normalized to 1000 events.

1043 of pileup on the efficiency of the CMS top tagger. With no additional pileup events, the efficiency of the
 1044 algorithm maintains its maximum value of $\sim 40\%$ up to jet p_T values of 1.2-1.3 TeV, at which point the
 1045 efficiency begins to fall to 10% or lower for jets with $p_T > 1.5$ TeV. With additional pileup events (and no
 1046 correction applied to the subjets), the efficiency degradation happens at much lower p_T values. The rate of
 1047 QCD jets passing the algorithm is also affected. With no additional pileup events, this mistag rate remains
 1048 below 5% over the entire range of jet p_T . After adding 140 pileup interactions to the simulated events, the
 1049 mistag rate from QCD jets increases to a maximum of 45% at a p_T of 500 GeV, though this can be reduced
 1050 through additional algorithm improvements.

1051 **Detector effects.** At large values of the top quark p_T , such as the region above 1.5 TeV at the LHC, QCD
 1052 radiation as well as the size of the detector elements become a limiting factor. In this regime, top quarks will
 1053 have hard radiations that may be identified as subjets and the top quark decay products become so highly
 1054 collimated that they cannot be individually resolved due to calorimeter detector segmentation and tracking
 1055 failures.

1056 The effects mentioned above cause a degradation in the top quark jet resolution at large p_T . For example,
 1057 the width of the top quark jet mass peak increases by a factor of two when comparing top quarks with
 1058 $p_T > 1.6$ TeV to those with $p_T > 0.8$ TeV, see Fig. 1-7. Algorithmic improvements extend the p_T range
 1059 where top jets can be reconstructed, but ultimately the granularity of individual calorimeter cells must be
 1060 increased to maintain a good top jet reconstruction.

1061 The reconstruction of top jets and substructure within large cone-size jets is a relatively new field that has
 1062 made tremendous progress in only a few years. More improvements are likely to come, especially as sizable
 1063 top quark event samples at the highest momenta become available at the LHC. The ultimate limit is expected
 1064 to come from the detector resolution, and future detectors such as for CLIC or VLHC machines will need
 1065 account for this.

1.7.3 Lepton colliders

A lepton collider (linear e^+e^- colliders ILC and CLIC and circular e^+e^- collider TLEP and the $\mu^+\mu^-$ collider) will allow for the study of electroweak production of $t\bar{t}$ pairs with no concurring QCD background. Linear colliders can use polarized beams, giving samples enriched in top quarks of left- or right-handed helicities. This can allow one to probe new physics scenarios predicting anomalous production rates of right-handed t quarks compared to the SM, and to disentangle the $t\gamma$ and tZ couplings, see Section 1.3.

Due to the electroweak production mechanism, all interesting processes occur at roughly the same rate, and backgrounds can easily be reduced to a negligible level. After applying selection cuts, it is possible to retain a signal sample of approximately 10^5 events at the 500 GeV linear collider with 500 fb^{-1} of integrated luminosity. Unlike at the LHC, there are no or few additional interactions (pileup) per beam crossing, especially for the ILC. Additional activity may come from $\gamma\gamma$ interactions. Ongoing studies show that this residual pile-up can be controlled when applying the invariant k_t jet algorithm [227, 228] for background suppression.

The lepton collider detectors are also more fine-grained and have better resolution than the LHC detectors. The charge of the b quark will be measured at a purity of 60% and better [109]. This is indispensable for the measurement of A_{FB}^t in fully hadronic decays, see Section 1.4. The jet energy resolution for LHC detectors is between 10% and 15% for jets below 100 GeV [229] whereas it is below 4% at the linear collider [21]. This results in a clean top quark sample with a narrow reconstructed mass as shown in Fig. 1-1.

Using A_{FB}^t , the top-Higgs coupling λ_t and the $t\bar{t}$ production cross section, electroweak couplings can be determined at the percent level. It is important that experimental and theoretical errors are kept at the same level. This requires a precise measurement of the luminosity and the beam polarization. Currently, both parameters are expected to be controlled to better than 0.5% at the linear collider. In general the realization of machine and detectors must not compromise the precision physics, which may be the biggest challenge in the coming years.

1.8 Conclusions

This is the concluding Section for top quark snowmass 2013 studies. We have discussed six topics – the top quark mass, top quark couplings to other SM particles; kinematics of top-like final states, rare decays of top quarks and top quark physics beyond the Standard Model. We will describe our conclusions for each of these topics.

We have argued that a theoretically clean measurement of the top mass to about 300 MeV is sufficient for many of the physics goals that are currently discussed, in particular electroweak precision fits. If no new physics is found at the LHC, it will be important to address the vacuum stability issue of the SM. To address this, a top mass measurement with a precision of 100 MeV is required, given the expected precision of the Higgs mass measurement. The top quark mass can be measured with an accuracy of about 500 MeV in individual measurements at the LHC, and their combination might reduce the uncertainty further. We note that both novel methods and the high-luminosity option are required for achieving this accuracy. The top mass can be measured with an accuracy of about 100 MeV (dominated by theoretical uncertainties) at a lepton collider, which matches well with the precision on the W mass achievable at such a facility.

While the LHC and a future linear collider provide complementary information on top quark couplings, there is no doubt that the LHC, especially the high-luminosity option, will probe a majority of top quark couplings to gluons, photons, Z 's, W 's and the Higgs boson with precision that should allow us to detect deviations

1107 caused by generic BSM physics at the TeV scale. The much higher precision achievable at a linear collider
1108 should then either allow us to study these deviations or exclude the existence of generic BSM physics at even
1109 higher scales, in particular for the γ and Z couplings. The top Yukawa coupling, one of the most important
1110 top couplings, will be measured to roughly equal precision at the LHC and the 500 GeV ILC and to better
1111 precision at a high-energy linear collider.

1112 Understanding how top quarks are produced and decay is an integral part of top physics at any collider.
1113 Kinematic distributions and differential cross sections are the key to achieving this goal. The measurement of
1114 basic top observables will help improve modeling of top quark events. The large top event samples available
1115 in the future will allow the study of new observables such as angular correlations or asymmetries that can
1116 uncover subtle new physics effects which may not be accessible otherwise.

1117 The LHC and a future linear collider are complementary in probing rare decays of the top quark. The LHC
1118 is better at probing flavor-changing couplings involving gluons, with about a factor two improvement in the
1119 branching ratio limits expected from the high-luminosity option. A linear collider is better for processes
1120 involving γ 's and Z 's. If rare decays are found, a linear collider also is able to probe the spin structure of
1121 the couplings involved.

1122 Top quarks play a very important role in searches for physics beyond the SM. In particular, solutions to
1123 the hierarchy problem require new particles decaying to top-like final states, such as stops in SUSY or top
1124 partners in other models. The LHC is able to cover the region of interest up to a few TeV in mass for stops,
1125 top-partners and resonances decaying into top quarks. The high-luminosity option extends the mass reach
1126 for these particles by roughly 50%. Given the current limits, only a multi-TeV lepton collider will be able
1127 to produce top partners and resonances directly. We note that there are stop models that might be difficult
1128 to discover at the LHC but can be probed at a linear collider, for example stealth stops.

1129 The 14 TeV LHC is a complex environment, especially the high pileup of the high-luminosity option which
1130 makes precision measurements of top mass, couplings and kinematic distributions challenging. Moreover,
1131 the 14 TeV LHC provides a large sample of boosted top quarks for the first time whose decay products can
1132 no longer be resolved using traditional methods. Our studies indicate that both of these challenges can be
1133 mitigated with algorithm developments and other improvements, many of which have not been deployed
1134 yet for these Snowmass studies in the high-luminosity scenario. The experimental environment at a lepton
1135 collider does not suffer from these problems and instead offers an ideal environment for precision top physics;
1136 there are few or no additional interactions per crossing and the detectors are more fine-grained and have
1137 better resolution.

1138 In summary, the high-luminosity LHC improves our knowledge of the top quark and extends the reach for
1139 new physics to interesting and relevant regions. A future lepton collider will be able to study the top quark
1140 in even more detail, in particular its mass and couplings. We are confident that the predictions in this report
1141 are conservative and that the experiments will do better with actual data than predicted here.

References

- 1142
- 1143 [1] CDF Collaboration. Observation of top quark production in $\bar{p}p$ collisions. *Phys.Rev.Lett.*, 74:2626–
1144 2631, 1995, hep-ex/9503002.
- 1145 [2] D0 Collaboration. Observation of the top quark. *Phys.Rev.Lett.*, 74:2632–2637, 1995, hep-ex/9503003.
- 1146 [3] Giuseppe Degrossi, Stefano Di Vita, Joan Elias-Miro, Jose R. Espinosa, Gian F. Giudice, et al. Higgs
1147 mass and vacuum stability in the Standard Model at NNLO. *JHEP*, 1208:098, 2012, 1205.6497.
- 1148 [4] M. Baak, M. Goebel, J. Haller, A. Hoecker, D. Kennedy, et al. The Electroweak Fit of the Standard
1149 Model after the Discovery of a New Boson at the LHC. *Eur.Phys.J.*, C72:2205, 2012, 1209.2716.
- 1150 [5] P. Janot, M. M. Bachtis, and A. Blondel. First Look at the Physics Case of TLEP. *TLEP report, in
1151 preparation*, 2013.
- 1152 [6] Katja Seidel, Frank Simon, Michal Tesar, and Stephane Poss. Top quark mass measurements at and
1153 above threshold at CLIC. 2013, 1303.3758.
- 1154 [7] Manel Martinez and Ramon Miquel. Multiparameter fits to the t anti-t threshold observables at a
1155 future e+ e- linear collider. *Eur.Phys.J.*, C27:49–55, 2003, hep-ph/0207315.
- 1156 [8] M. Vos et al. Top quark mass measurement at the ILC. *Snowmass 2013 whitepaper, in preparation*,
1157 2013.
- 1158 [9] Martin Beneke, Yuichiro Kiyo, and Kurt Schuller. NNNLO results on top-quark pair production near
1159 threshold. *PoS, RADCOR2007:051*, 2007, 0801.3464.
- 1160 [10] James S. Gainer, Joseph Lykken, Konstantin T. Matchev, Stephen Mrenna, and Myeonghun Park.
1161 The Matrix Element Method: Past, Present, and Future. 2013, 1307.3546.
- 1162 [11] ATLAS Collaboration. Measurement of the top quark mass with the template method in the $t\bar{t}$ lepton
1163 + jets channel using ATLAS data. *Eur.Phys.J.*, C72:2046, 2012, 1203.5755.
- 1164 [12] CMS Collaboration. Measurement of the top-quark mass in $t\bar{t}$ events with lepton+jets final states in
1165 pp collisions at $\sqrt{s} = 7$ TeV. *JHEP*, 1212:105, 2012, 1209.2319.
- 1166 [13] CMS Collaboration. Measurement of masses in the $t\bar{t}$ system by kinematic endpoints in pp collisions
1167 at $\sqrt{s}=7$ TeV. 2013, 1304.5783.
- 1168 [14] Avto Kharchilava. Top mass determination in leptonic final states with J/ψ . *Phys.Lett.*, B476:73–78,
1169 2000, hep-ph/9912320.
- 1170 [15] Ansgar Denner, Stefan Dittmaier, Stefan Kallweit, and Stefano Pozzorini. NLO QCD corrections
1171 to off-shell top-antitop production with leptonic decays at hadron colliders. *JHEP*, 1210:110, 2012,
1172 1207.5018.
- 1173 [16] Giuseppe Bevilacqua, Michal Czakon, Andreas van Hameren, Costas G. Papadopoulos, and Malgorzata
1174 Worek. Complete off-shell effects in top quark pair hadroproduction with leptonic decay at next-to-
1175 leading order. *JHEP*, 1102:083, 2011, 1012.4230.
- 1176 [17] ATLAS collaboration. Measurement of the Top Quark Mass from $\sqrt{s} = 7$ TeV ATLAS data using a
1177 3-dimensional template fit. *ATLAS-CONF-2013-046*, 2013.
- 1178 [18] Sandip Biswas, Kirill Melnikov, and Markus Schulze. Next-to-leading order QCD effects and the top
1179 quark mass measurements at the LHC. *JHEP*, 1008:048, 2010, 1006.0910.

- 1180 [19] Simone Alioli, Patricia Fernandez, Juan Fuster, Adrian Irlles, Sven-Olaf Moch, et al. A new observable
1181 to measure the top-quark mass at hadron colliders. *Eur.Phys.J.*, C73:2438, 2013, 1303.6415.
- 1182 [20] D0 Collaboration. An Improved determination of the width of the top quark. *Phys.Rev.*, D85:091104,
1183 2012, 1201.4156.
- 1184 [21] Howard Baer, Tim Barklow, Keisuke Fujii, Yuanning Gao, Andre Hoang, et al. The International
1185 Linear Collider Technical Design Report - Volume 2: Physics. 2013, 1306.6352.
- 1186 [22] A. Juste, Y. Kiyo, F. Petriello, T. Teubner, K. Agashe, et al. Report of the 2005 Snowmass top/QCD
1187 working group. 2006, hep-ph/0601112.
- 1188 [23] J.A. Aguilar-Saavedra. A Minimal set of top anomalous couplings. *Nucl.Phys.*, B812:181–204, 2009,
1189 0811.3842.
- 1190 [24] Cen Zhang and Scott Willenbrock. Effective Field Theory for Top Quark Physics. *Nuovo Cim.*,
1191 C033N4:285–291, 2010, 1008.3155.
- 1192 [25] Michal Czakon, Paul Fiedler, and Alexander Mitov. The total top quark pair production cross-section
1193 at hadron colliders through $O(\alpha_s^4)$. 2013, 1303.6254.
- 1194 [26] Peter Baernreuther, Michal Czakon, and Alexander Mitov. Percent Level Precision Physics at the
1195 Tevatron: First Genuine NNLO QCD Corrections to $q\bar{q} \rightarrow t\bar{t} + X$. *Phys.Rev.Lett.*, 109:132001, 2012,
1196 1204.5201.
- 1197 [27] Michal Czakon and Alexander Mitov. NNLO corrections to top-pair production at hadron colliders:
1198 the all-fermionic scattering channels. *JHEP*, 1212:054, 2012, 1207.0236.
- 1199 [28] J.H. Khn, A. Scharf, and P. Uwer. Weak Interactions in Top-Quark Pair Production at Hadron
1200 Colliders: An Update. 2013, 1305.5773.
- 1201 [29] Matthew Baumgart and Brock Tweedie. A New Twist on Top Quark Spin Correlations. *JHEP*,
1202 1303:117, 2013, 1212.4888.
- 1203 [30] M Baumgart, A Loginov, A Garcia-Bellido, and J Adelman. Summary of “Top couplings” High Energy
1204 Frontier Study Group. 2013.
- 1205 [31] ATLAS Collaboration. Measurement of the top quark pair production cross section in the single-lepton
1206 channel with atlas in proton-proton collisions at 8 tev using kinematic fits with b-tagging. Technical
1207 Report ATLAS-CONF-2012-149, CERN, Geneva, Nov 2012.
- 1208 [32] ATLAS and CMS Collaborations. Combination of atlas and cms top-quark pair cross section
1209 measurements using up to 1.1 fb-1 of data at 7 tev. Technical Report ATLAS-CONF-2012-134, CMS-
1210 PAS-TOP-12-003, CERN, Geneva, Sep 2012.
- 1211 [33] CMS Collaboration. Top pair cross section in dileptons. Technical Report CMS-PAS-TOP-12-007,
1212 CERN, Geneva, 2012.
- 1213 [34] ATLAS Collaboration. Measurement of the t -channel single top-quark production cross section in pp
1214 collisions at $\sqrt{s} = 7$ TeV with the ATLAS detector. *Phys.Lett.*, B717:330–350, 2012, 1205.3130.
- 1215 [35] ATLAS Collaboration. Measurement of t -channel single top-quark production in pp collisions at \sqrt{s}
1216 = 8 tev with the atlas detector. Technical Report ATLAS-CONF-2012-132, CERN, Geneva, Sep 2012.
- 1217 [36] CMS Collaboration. Measurement of the single-top-quark t -channel cross section in pp collisions at
1218 $\sqrt{s} = 7$ TeV. *JHEP*, 1212:035, 2012, 1209.4533.

- 1219 [37] CMS Collaboration. Measurement of the single-top t-channel cross section in pp collisions at centre-
1220 of-mass energy of 8 tev. Technical Report CMS-PAS-TOP-12-011, CERN, Geneva, 2012.
- 1221 [38] Nikolaos Kidonakis. NNLL threshold resummation for top-pair and single-top production. 2012,
1222 1210.7813.
- 1223 [39] ATLAS Collaboration. Evidence for the associated production of a W boson and a top quark in ATLAS
1224 at $\sqrt{s} = 7$ TeV. *Phys.Lett.*, B716:142–159, 2012, 1205.5764.
- 1225 [40] CMS Collaboration. Evidence for associated production of a single top quark and W boson in pp
1226 collisions at 7 TeV. *Phys.Rev.Lett.*, 2012, 1209.3489.
- 1227 [41] CMS Collaboration. Observation of associated production of a single top quark and w boson in pp
1228 collisions at $\text{sqrt}(s) = 8$ tev. Technical Report CMS-PAS-TOP-12-040, CERN, Geneva, 2013.
- 1229 [42] Nicola Cabibbo. Unitary Symmetry and Leptonic Decays. *Phys.Rev.Lett.*, 10:531–533, 1963.
- 1230 [43] Andrzej Czarnecki, Jurgen G. Korner, and Jan H. Piclum. Helicity fractions of W bosons from top
1231 quark decays at NNLO in QCD. *Phys.Rev.*, D81:111503, 2010, 1005.2625.
- 1232 [44] Jun Gao, Chong Sheng Li, and Hua Xing Zhu. Top Quark Decay at Next-to-Next-to Leading Order
1233 in QCD. *Phys.Rev.Lett.*, 110:042001, 2013, 1210.2808.
- 1234 [45] Mathias Brucherseifer, Fabrizio Caola, and Kirill Melnikov. $\mathcal{O}(\alpha_s^2)$ corrections to fully-differential top
1235 quark decays. *JHEP*, 1304:059, 2013, 1301.7133.
- 1236 [46] H. Lacker, A. Menzel, F. Spettel, D. Hirschebuhl, J. Luck, et al. Model-independent extraction of
1237 $|V_{tq}|$ matrix elements from top-quark measurements at hadron colliders. *Eur.Phys.J.*, C72:2048, 2012,
1238 1202.4694.
- 1239 [47] B. Schoenrock, E. Druke, B. Alvarez Gonzalez, and R. Schwienhorst. Single top quark cross section
1240 measurement in the t-channel at the high-luminosity LHC. 2013.
- 1241 [48] ATLAS Collaboration. Search for \mathcal{CP} violation in single top quark events in pp collisions at $\sqrt{s} = 7$
1242 tev with the atlas detector. Technical Report ATLAS-CONF-2013-032, CERN, Geneva, 2013.
- 1243 [49] E. Boos, M. Dubinin, A. Pukhov, M. Sachwitz, and H.J. Schreiber. Single top production in $e^+ e^-$, e^-
1244 e^- , gamma e and gamma gamma collisions. *Eur.Phys.J.*, C21:81–91, 2001, hep-ph/0104279.
- 1245 [50] Sukanta Dutta, Ashok Goyal, Mukesh Kumar, and Bruce Mellado. Measuring anomalous Wtb couplings
1246 at e^-p collider. 2013, 1307.1688.
- 1247 [51] ATLAS Collaboration. Measurement of the top quark charge in pp collisions at $\text{sqrt}(s) = 7$ TeV with
1248 the ATLAS detector. 2013, 1307.4568.
- 1249 [52] ATLAS Collaboration. Measurement of the inclusive t bar gamma cross section with the atlas detector.
1250 Technical Report ATLAS-CONF-2011-153, CERN, Geneva, Nov 2011.
- 1251 [53] U. Baur, A. Juste, D. Rainwater, and L.H. Orr. Improved measurement of ttZ couplings at the CERN
1252 LHC. *Phys.Rev.*, D73:034016, 2006, hep-ph/0512262.
- 1253 [54] U. Baur, A. Juste, L.H. Orr, and D. Rainwater. Probing electroweak top quark couplings at hadron
1254 colliders. *Phys.Rev.*, D71:054013, 2005, hep-ph/0412021.
- 1255 [55] Achilleas Lazopoulos, Thomas McElmurry, Kirill Melnikov, and Frank Petriello. Next-to-leading order
1256 QCD corrections to ttZ production at the LHC. *Phys.Lett.*, B666:62–65, 2008, 0804.2220.

- 1257 [56] Kirill Melnikov, Markus Schulze, and Andreas Scharf. QCD corrections to top quark pair production
1258 in association with a photon at hadron colliders. *Phys.Rev.*, D83:074013, 2011, 1102.1967.
- 1259 [57] M.V. Garzelli, A. Kardos, C.G. Papadopoulos, and Z. Trocsanyi. $t \bar{t} W^{+-}$ and $t \bar{t} Z$ Hadroproduction
1260 at NLO accuracy in QCD with Parton Shower and Hadronization effects. *JHEP*, 1211:056, 2012,
1261 1208.2665.
- 1262 [58] M.V. Garzelli, A. Kardos, C.G. Papadopoulos, and Z. Trocsanyi. $Z0$ - boson production in association
1263 with a top anti-top pair at NLO accuracy with parton shower effects. *Phys.Rev.*, D85:074022, 2012,
1264 1111.1444.
- 1265 [59] John Campbell, R. Keith Ellis, and Raoul Rntsch. Single top production in association with a Z boson
1266 at the LHC. 2013, 1302.3856.
- 1267 [60] CMS Collaboration. Cms at the high-energy frontier. contribution to the update of the european
1268 strategy for particle physics. Technical Report CMS-NOTE-2012-006. CERN-CMS-NOTE-2012-006,
1269 CERN, Geneva, Oct 2012.
- 1270 [61] ATLAS Collaboration. Physics at a high-luminosity lhc with atlas (update). Technical Report ATL-
1271 PHYS-PUB-2012-004, CERN, Geneva, Oct 2012.
- 1272 [62] J. Vasquez and J. Adelman. Measurement of Higgs-muon coupling in $t\bar{t}H$ at the high-luminosity LHC.
1273 2013.
- 1274 [63] Ryo Yonamine, Katsumasa Ikematsu, Tomohiko Tanabe, Keisuke Fujii, Yuichiro Kiyoy, et al. Measuring
1275 the top Yukawa coupling at the ILC at $\sqrt{s} = 500$ GeV. *Phys.Rev.*, D84:014033, 2011, 1104.5132.
- 1276 [64] CLIC Detector and Physics Study Collaboration. Physics at the CLIC e+e- Linear Collider – Input
1277 to the Snowmass process 2013. 2013, 1307.5288.
- 1278 [65] Kirill Melnikov and Markus Schulze. NLO QCD corrections to top quark pair production and decay
1279 at hadron colliders. *JHEP*, 0908:049, 2009, 0907.3090.
- 1280 [66] John M. Campbell and R. Keith Ellis. Top-quark processes at NLO in production and decay. 2012,
1281 1204.1513.
- 1282 [67] Kirill Melnikov and Markus Schulze. NLO QCD corrections to top quark pair production in association
1283 with one hard jet at hadron colliders. *Nucl.Phys.*, B840:129–159, 2010, 1004.3284.
- 1284 [68] S. Dittmaier, P. Uwer, and S. Weinzierl. Hadronic top-quark pair production in association with a
1285 hard jet at next-to-leading order QCD: Phenomenological studies for the Tevatron and the LHC. *Eur.*
1286 *Phys. J.*, C59:625–646, 2009, 0810.0452.
- 1287 [69] Adam Kardos, Costas Papadopoulos, and Zoltan Trocsanyi. Top quark pair production in association
1288 with a jet with NLO parton showering. *Phys.Lett.*, B705:76–81, 2011, 1101.2672.
- 1289 [70] John M. Campbell and R.K. Ellis. MCFM for the Tevatron and the LHC. *Nucl.Phys.Proc.Suppl.*,
1290 205-206:10–15, 2010, 1007.3492.
- 1291 [71] J. Shelton A. Jung, M. Schulze. Kinematics of Top Quark Final States. *Snowmass 2013 whitepaper,*
1292 *in preparation*, 2013.
- 1293 [72] Valentin Ahrens, Andrea Ferroglia, Matthias Neubert, Ben D. Pecjak, and Li-Lin Yang. RG-improved
1294 single-particle inclusive cross sections and forward-backward asymmetry in $t\bar{t}$ production at hadron
1295 colliders. *JHEP*, 1109:070, 2011, 1103.0550.

- 1296 [73] B. Auerbach, S.V. Chekanov, and N. Kidonakis. Studies of highly-boosted top quarks near the TeV
1297 scale using jet masses at the LHC. 2013, 1301.5810. arXiv:1301.5810. Also as SNOW13-00027.
- 1298 [74] D0 Collaboration. Evidence for spin correlation in $t\bar{t}$ production. *Phys.Rev.Lett.*, 108:032004, 2012,
1299 1110.4194.
- 1300 [75] ATLAS Collaboration. Observation of spin correlation in $t\bar{t}$ events from pp collisions at $\sqrt{s} = 7$
1301 TeV using the ATLAS detector. *Phys.Rev.Lett.*, 108:212001, 2012, 1203.4081.
- 1302 [76] CMS Collaboration. Measurement of spin correlations in $t\bar{t}$ production. Technical Report CMS-
1303 PAS-TOP-12-004, CERN, Geneva, 2012.
- 1304 [77] Gregory Mahlon and Stephen J. Parke. Spin Correlation Effects in Top Quark Pair Production at the
1305 LHC. *Phys.Rev.*, D81:074024, 2010, 1001.3422.
- 1306 [78] Werner Bernreuther and Zong-Guo Si. Distributions and correlations for top quark pair production
1307 and decay at the Tevatron and LHC. *Nucl.Phys.*, B837:90–121, 2010, 1003.3926.
- 1308 [79] Stefano Frixione, Eric Laenen, Patrick Motylinski, and Bryan R. Webber. Angular correlations of
1309 lepton pairs from vector boson and top quark decays in Monte Carlo simulations. *JHEP*, 0704:081,
1310 2007, hep-ph/0702198.
- 1311 [80] Zhenyu Han, Andrey Katz, David Krohn, and Matthew Reece. (Light) Stop Signs. *JHEP*, 1208:083,
1312 2012, 1205.5808.
- 1313 [81] Werner Bernreuther and Zong-Guo Si. Top quark spin correlations and polarization at the LHC:
1314 standard model predictions and effects of anomalous top chromo moments. 2013, 1305.2066.
- 1315 [82] Matthew Baumgart and Brock Tweedie. Discriminating Top-Antitop Resonances using Azimuthal
1316 Decay Correlations. *JHEP*, 1109:049, 2011, 1104.2043.
- 1317 [83] Fabrizio Caola, Kirill Melnikov, and Markus Schulze. A complete next-to-leading order QCD
1318 description of resonant Z' production and decay into $t\bar{t}$ final states. *Phys.Rev.*, D87:034015, 2013,
1319 1211.6387.
- 1320 [84] Johann H. Kuhn and German Rodrigo. Charge asymmetry in hadroproduction of heavy quarks.
1321 *Phys.Rev.Lett.*, 81:49–52, 1998, hep-ph/9802268.
- 1322 [85] Johann H. Kuhn and German Rodrigo. Charge asymmetry of heavy quarks at hadron colliders.
1323 *Phys.Rev.*, D59:054017, 1999, hep-ph/9807420.
- 1324 [86] Leandro G. Almeida, George Sterman, and Werner Vogelsang. Threshold resummation for the top
1325 quark charge asymmetry. *Phys. Rev. D*, 78:014008, Jul 2008.
- 1326 [87] Oscar Antuñano, Johann H. Kühn, and Germán Rodrigo. Top quarks, axigluons, and charge
1327 asymmetries at hadron colliders. *Phys. Rev. D*, 77:014003, Jan 2008.
- 1328 [88] M. T. Bowen, S. D. Ellis, and D. Rainwater. Standard model top quark asymmetry at the fermilab
1329 tevatron. *Phys. Rev. D*, 73:014008, Jan 2006.
- 1330 [89] CDF Collaboration. Measurement of the top quark forward-backward production asymmetry and its
1331 dependence on event kinematic properties. *Phys. Rev. D*, 87:092002, May 2013.
- 1332 [90] D0 Collaboration. Measurement of leptonic asymmetries and top-quark polarization in $t\bar{t}$ production.
1333 *Phys. Rev. D*, 87:011103, Jan 2013.

- 1334 [91] ATLAS Collaboration. Measurement of the charge asymmetry in top quark pair production in pp
1335 collisions at $\sqrt{s} = 7$ TeV using the ATLAS detector. *Eur.Phys.J.*, C72:2039, 2012, 1203.4211.
- 1336 [92] CMS Collaboration. Measurement of the charge asymmetry in top-quark pair production in proton-
1337 proton collisions at. *Physics Letters B*, 709(12):28 – 49, 2012.
- 1338 [93] Werner Bernreuther and Zong-Guo Si. Top quark and leptonic charge asymmetries for the tevatron
1339 and lhc. *Phys. Rev. D*, 86:034026, Aug 2012.
- 1340 [94] ATLAS Collaboration. Measurement of the charge asymmetry in dileptonic decay of top quark pairs in
1341 pp collisions at $s = 7$ tev using the atlas detector. Technical Report ATLAS-CONF-2012-057, CERN,
1342 Geneva, Jun 2012.
- 1343 [95] CMS Collaboration. Top charge asymmetry measurement in dileptons at 7 tev. Technical Report
1344 CMS-PAS-TOP-12-010, CERN, Geneva, 2012.
- 1345 [96] R Gauld, on behalf of the LHCb Collaboration. Measuring top quark production asymmetries at lhcb.
1346 *LHCb-PUB-2013-009*, 2013.
- 1347 [97] Alexander L. Kagan, Jernej F. Kamenik, Gilad Perez, and Sheldon Stone. Top LHCb Physics.
1348 *Phys.Rev.Lett.*, 107:082003, 2011, 1103.3747.
- 1349 [98] Paul H. Frampton, Jing Shu, and Kai Wang. Axigluon as Possible Explanation for p anti-p -i t anti-t
1350 Forward-Backward Asymmetry. *Phys.Lett.*, B683:294–297, 2010, 0911.2955.
- 1351 [99] Yang Bai, JoAnne L. Hewett, Jared Kaplan, and Thomas G. Rizzo. LHC Predictions from a Tevatron
1352 Anomaly in the Top Quark Forward-Backward Asymmetry. *JHEP*, 1103:003, 2011, 1101.5203.
- 1353 [100] Gustavo Marques Tavares and Martin Schmaltz. Explaining the t-tbar asymmetry with a light axigluon.
1354 *Phys.Rev.*, D84:054008, 2011, 1107.0978.
- 1355 [101] Moira Gresham, Jessie Shelton, and Kathryn M. Zurek. Open windows for a light axigluon explanation
1356 of the top forward-backward asymmetry. *JHEP*, 1303:008, 2013, 1212.1718.
- 1357 [102] Ulrich Haisch and Susanne Westhoff. Massive Color-Octet Bosons: Bounds on Effects in Top-Quark
1358 Pair Production. *JHEP*, 1108:088, 2011, 1106.0529.
- 1359 [103] Stefan Berge and Susanne Westhoff. Top-Quark Charge Asymmetry Goes Forward: Two New
1360 Observables for Hadron Colliders. 2013, 1305.3272.
- 1361 [104] Stefan Berge and Susanne Westhoff. Charge Asymmetry in Top Pair plus Jet Production. 2013,
1362 1307.6225.
- 1363 [105] Edmond L. Berger, Qing-Hong Cao, Chuan-Ren Chen, Jiang-Hao Yu, and Hao Zhang. The Top Quark
1364 Production Asymmetries A_{FB}^t and A_{FB}^ℓ . *Phys.Rev.Lett.*, 108:072002, 2012, 1201.1790.
- 1365 [106] M.S. Amjad et al. A precise determination of top quark electroweak couplings at the ILC operating
1366 at $\sqrt{s} = 500$ GeV. *LC-REP-2013-007*, 2013.
- 1367 [107] Wolfgang Kilian, Thorsten Ohl, and Jurgen Reuter. WHIZARD: Simulating Multi-Particle Processes
1368 at LHC and ILC. *Eur.Phys.J.*, C71:1742, 2011, 0708.4233.
- 1369 [108] Mauro Moretti, Thorsten Ohl, and Jurgen Reuter. O’Mega: An Optimizing matrix element generator.
1370 *IKDA-2001-06, LC-TOOL-2001-040, hep-ph/0102195*, 2001, hep-ph/0102195.

- 1371 [109] Erik Devetak, Andrei Nomerotski, and Michael Peskin. Top quark anomalous couplings at the
1372 International Linear Collider. *Phys.Rev.*, D84:034029, 2011, 1005.1756.
- 1373 [110] A.H. Hoang, M. Beneke, K. Melnikov, T. Nagano, A. Ota, et al. Top - anti-top pair production close
1374 to threshold: Synopsis of recent NNLO results. *Eur.Phys.J.direct*, C2:1, 2000, hep-ph/0001286.
- 1375 [111] N. Craig and M. Velasco. Top Rare Decays. *Snowmass whitepaper, in preparation*, 2013.
- 1376 [112] J.A. Aguilar-Saavedra. Top flavor-changing neutral interactions: Theoretical expectations and
1377 experimental detection. *Acta Phys.Polon.*, B35:2695–2710, 2004, hep-ph/0409342.
- 1378 [113] David Atwood, Laura Reina, and Amarjit Soni. Phenomenology of two Higgs doublet models with
1379 flavor changing neutral currents. *Phys.Rev.*, D55:3156–3176, 1997, hep-ph/9609279.
- 1380 [114] Santi Bejar. Flavor changing neutral decay effects in models with two Higgs boson doublets:
1381 Applications to LHC Physics. 2006, hep-ph/0606138.
- 1382 [115] J.J. Cao, G. Eilam, M. Frank, K. Hikasa, G.L. Liu, et al. SUSY-induced FCNC top-quark processes
1383 at the large hadron collider. *Phys.Rev.*, D75:075021, 2007, hep-ph/0702264.
- 1384 [116] Jin Min Yang, Bing-Lin Young, and X. Zhang. Flavor changing top quark decays in r parity violating
1385 SUSY. *Phys.Rev.*, D58:055001, 1998, hep-ph/9705341.
- 1386 [117] G. Eilam, A. Gemintern, Tao Han, J.M. Yang, and X. Zhang. Top quark rare decay $t \rightarrow ch$ in R -parity
1387 violating SUSY. *Phys.Lett.*, B510:227–235, 2001, hep-ph/0102037.
- 1388 [118] Kaustubh Agashe, Gilad Perez, and Amarjit Soni. Collider Signals of Top Quark Flavor Violation
1389 from a Warped Extra Dimension. *Phys.Rev.*, D75:015002, 2007, hep-ph/0606293.
- 1390 [119] Kaustubh Agashe and Roberto Contino. Composite Higgs-Mediated FCNC. *Phys.Rev.*, D80:075016,
1391 2009, 0906.1542.
- 1392 [120] G. Eilam, J.L. Hewett, and A. Soni. Rare decays of the top quark in the standard and two Higgs
1393 doublet models. *Phys.Rev.*, D44:1473–1484, 1991.
- 1394 [121] B. Mele, S. Petrarca, and A. Soddu. A New evaluation of the $t \rightarrow cH$ decay width in the standard model.
1395 *Phys.Lett.*, B435:401–406, 1998, hep-ph/9805498.
- 1396 [122] Michael E. Luke and Martin J. Savage. Flavor changing neutral currents in the Higgs sector and rare
1397 top decays. *Phys.Lett.*, B307:387–393, 1993, hep-ph/9303249.
- 1398 [123] CMS Collaboration. Search for flavor changing neutral currents in top quark decays in pp collisions at
1399 7 TeV. *Phys.Lett.*, B718:1252–1272, 2013, 1208.0957.
- 1400 [124] ATLAS Collaboration. Search for FCNC single top-quark production at $\sqrt{s} = 7$ TeV with the ATLAS
1401 detector. *Phys.Lett.*, B712:351–369, 2012, 1203.0529.
- 1402 [125] CDF Collaboration. Search for flavor-changing neutral current decays of the top quark in $p\bar{p}$ collisions
1403 at $\sqrt{s} = 1.8$ TeV. *Phys.Rev.Lett.*, 80:2525–2530, 1998.
- 1404 [126] CDF Collaboration. Search for Invisible Top Decays with 1.9 fb⁻¹ of CDF-II Data.
1405 *CDF/PUB/TOP/PUBLIC/9496*, 2008.
- 1406 [127] H1 Collaboration. Search for Single Top Quark Production at HERA. *Phys.Lett.*, B678:450–458, 2009,
1407 0904.3876.

- 1408 [128] Nathaniel Craig, Jared A. Evans, Richard Gray, Michael Park, Sunil Somalwar, et al. Searching for
1409 $t \rightarrow ch$ with Multi-Leptons. *Phys.Rev.*, D86:075002, 2012, 1207.6794.
- 1410 [129] ATLAS Collaboration. A search for flavour changing neutral currents in top-quark decays in pp collision
1411 data collected with the ATLAS detector at $\sqrt{s} = 7$ TeV. *JHEP*, 1209:139, 2012, 1206.0257.
- 1412 [130] Patrick J. Fox, Zoltan Ligeti, Michele Papucci, Gilad Perez, and Matthew D. Schwartz. Deciphering
1413 top flavor violation at the LHC with B factories. *Phys.Rev.*, D78:054008, 2008, 0704.1482.
- 1414 [131] Roni Harnik, Joachim Kopp, and Jure Zupan. Flavor Violating Higgs Decays. *JHEP*, 1303:026, 2013,
1415 1209.1397.
- 1416 [132] ATLAS Collaboration. Physics at a High-Luminosity LHC with ATLAS. *ATL-PHYS-PUB-2012-001*,
1417 2013.
- 1418 [133] J.A. Aguilar-Saavedra and T. Riemann. Probing top flavor changing neutral couplings at TESLA.
1419 2001, hep-ph/0102197.
- 1420 [134] N. Craig. . *private communication*, 2013.
- 1421 [135] Jun Gao, Chong Sheng Li, Li Lin Yang, and Hao Zhang. Search for anomalous top quark production
1422 at the early LHC. *Phys.Rev.Lett.*, 107:092002, 2011, 1104.4945.
- 1423 [136] Tao Han and JoAnne L. Hewett. Top charm associated production in high-energy e^+e^- collisions.
1424 *Phys.Rev.*, D60:074015, 1999, hep-ph/9811237.
- 1425 [137] CMS Collaboration. Measurement of the ratio $b(t \text{ to } wb)/b(t \text{ to } wq)$. Technical Report CMS-PAS-
1426 TOP-12-035, CERN, Geneva, 2013.
- 1427 [138] J.A. Aguilar-Saavedra and A. Onofre. Using single top rapidity to measure V_{td} , V_{ts} , V_{tb} at hadron
1428 colliders. *Phys.Rev.*, D83:073003, 2011, 1002.4718.
- 1429 [139] Stephen P. Martin. A Supersymmetry primer. 1997, hep-ph/9709356.
- 1430 [140] Martin Schmaltz and David Tucker-Smith. Little Higgs review. *Ann.Rev.Nucl.Part.Sci.*, 55:229–270,
1431 2005, hep-ph/0502182.
- 1432 [141] Maxim Perelstein. Little Higgs models and their phenomenology. *Prog.Part.Nucl.Phys.*, 58:247–291,
1433 2007, hep-ph/0512128.
- 1434 [142] Hooman Davoudiasl, Shrihari Gopalakrishna, Eduardo Ponton, and Jose Santiago. Warped 5-
1435 Dimensional Models: Phenomenological Status and Experimental Prospects. *New J.Phys.*, 12:075011,
1436 2010, 0908.1968.
- 1437 [143] Roberto Contino. The Higgs as a Composite Nambu-Goldstone Boson. 2010, 1005.4269.
- 1438 [144] Y. Gershtein, M. Luty, M. Narain, L. Wang, and D. (conveners) Whiteson. The Path Beyond the
1439 Standard Model. *Snowmass report, in preparation*, 2013.
- 1440 [145] ATLAS Collaboration. Search for direct production of the top squark in the all-hadronic $t\bar{t} + \text{etmiss}$
1441 final state in 21 fb⁻¹ of p-p collisions at $\sqrt{s}=8$ TeV with the ATLAS detector. *ATLAS-CONF-2013-*
1442 *024*, 2013.
- 1443 [146] CMS Collaboration. Search for top-squark pair production in the single lepton final state in pp collisions
1444 at 8 TeV. *CMS-PAS-SUS-13-011*, 2013.

- 1445 [147] ATLAS Collaboration. Searches for Supersymmetry at the high luminosity LHC with the ATLAS
1446 Detector. *ATL-PHYS-PUB-2013-002*. [European strategy study; update with their Snowmass white
1447 paper when available], 2013.
- 1448 [148] Jim Olson. . talk at the Seattle energy frontier workshop [replace with CMS white paper reference when
1449 available], 2013.
- 1450 [149] Tilman Plehn, Michael Spannowsky, Michihisa Takeuchi, and Dirk Zerwas. Stop Reconstruction with
1451 Tagged Tops. *JHEP*, 1010:078, 2010, 1006.2833.
- 1452 [150] Tilman Plehn, Michael Spannowsky, and Michihisa Takeuchi. Stop searches in 2012. *JHEP*, 1208:091,
1453 2012, 1205.2696.
- 1454 [151] David E. Kaplan, Keith Rehermann, and Daniel Stolarski. Searching for Direct Stop Production in
1455 Hadronic Top Data at the LHC. *JHEP*, 1207:119, 2012, 1205.5816.
- 1456 [152] Bhaskar Dutta, Teruki Kamon, Nikolay Kolev, Kuver Sinha, and Kechen Wang. Searching for Top
1457 Squarks at the LHC in Fully Hadronic Final State. *Phys.Rev.*, D86:075004, 2012, 1207.1873.
- 1458 [153] D. Stolarski. Reach in All Hadronic Stop Decays. *Snowmass white paper, in preparation*, 2013.
- 1459 [154] Z Ha and A Katz. Stealth Stops. *Snowmass white paper, in preparation*, 2013.
- 1460 [155] Can Kilic and Brock Tweedie. Cornering Light Stops with Dileptonic mT2. *JHEP*, 1304:110, 2013,
1461 1211.6106.
- 1462 [156] A. G. et al. Delannoy. Probing Stealthy, Compressed, and Light Stops with Vector Boson Fusion at
1463 the LHC. *Snowmass white paper, in preparation*, 2013.
- 1464 [157] Christopher Brust, Andrey Katz, Scott Lawrence, and Raman Sundrum. SUSY, the Third Generation
1465 and the LHC. *JHEP*, 1203:103, 2012, 1110.6670.
- 1466 [158] ATLAS Collaboration. Search for strong production of supersymmetric particles in final states with
1467 missing transverse momentum and at least three b-jets using 20.1 fb^{-1} of pp collisions at $\sqrt{s} = 8$
1468 TeV with the ATLAS Detector. *ATLAS-CONF-2013-061*, 2013.
- 1469 [159] CMS Collaboration. Search for Supersymmetry in pp collisions at 8 TeV in events with a single lepton,
1470 multiple jets and b-tags. *CMS-PAS-SUS-13-007*, 2013.
- 1471 [160] Joshua Berger, Maxim Perelstein, Michael Saelim, and Andrew Spray. Boosted Tops from Gluino
1472 Decays. 2011, 1111.6594.
- 1473 [161] M. Graesser. Asymmetric Stop Decays and Topness at the 14 TeV LHC. *Snowmass white paper, in*
1474 *preparation*, 2013.
- 1475 [162] Michael L. Graesser and Jessie Shelton. Hunting Asymmetric Stops. 2012, 1212.4495.
- 1476 [163] B. et al. Dutta. Top Squark Searches and Well-Tempered Bino/Higgsino Dark Matter at the LHC.
1477 *Snowmass white paper, in preparation*, 2013.
- 1478 [164] N. Arkani-Hamed, A. Delgado, and G.F. Giudice. The Well-tempered neutralino. *Nucl.Phys.*,
1479 B741:108–130, 2006, hep-ph/0601041.
- 1480 [165] Emanuel Nikolidakis and Christopher Smith. Minimal Flavor Violation, Seesaw, and R-parity.
1481 *Phys.Rev.*, D77:015021, 2008, 0710.3129.

- 1482 [166] Csaba Csaki, Yuval Grossman, and Ben Heidenreich. MFV SUSY: A Natural Theory for R-Parity
1483 Violation. *Phys.Rev.*, D85:095009, 2012, 1111.1239.
- 1484 [167] D. Duggan, J. A. Evans, J. Hirschauer, K. Kaadze, A. Lath, and M. Walker. Sensitivity of an Upgraded
1485 LHC to R-Parity Violating Signatures of the MSSM. *Snowmass white paper, in preparation*, 2013.
- 1486 [168] Joshua Berger, Maxim Perelstein, Michael Saelim, and Philip Tanedo. The Same-Sign Dilepton
1487 Signature of RPV/MFV SUSY. *JHEP*, 1304:077, 2013, 1302.2146.
- 1488 [169] Zhenyu Han, Andrey Katz, Minho Son, and Brock Tweedie. Boosting Searches for Natural SUSY with
1489 RPV via Gluino Cascades. 2012, 1211.4025.
- 1490 [170] A. Katz. Search for RPV Gluino in RPV Natural SUSY. *Snowmass white paper, in preparation*, 2013.
- 1491 [171] Jan Mrazek and Andrea Wulzer. A Strong Sector at the LHC: Top Partners in Same-Sign Dileptons.
1492 *Phys.Rev.*, D81:075006, 2010, 0909.3977.
- 1493 [172] Kaustubh Agashe, Roberto Contino, Leandro Da Rold, and Alex Pomarol. A Custodial symmetry for
1494 Zb anti-b. *Phys.Lett.*, B641:62–66, 2006, hep-ph/0605341.
- 1495 [173] CMS Collaboration. Search for T5/3 top partners in same-sign dilepton final state. 2013.
- 1496 [174] ATLAS Collaboration. Search for exotic same-sign dilepton signatures (b' quark, T_5/3 and four top
1497 quarks production) in 4.7/fb of pp collisions at sqrt(s)=7 TeV with the ATLAS detector. 2012.
- 1498 [175] S. Bhattacharya, J. George, U. Heintz, A. Kumar, M. Narain, and J. Stupak. Prospects for Heavy
1499 Vector-like Charge 2/3 Quarks at the LHC with $\sqrt{s} = 14$ and 33 TeV. *Snowmass white paper, in*
1500 *preparation*, 2013.
- 1501 [176] T. Andeen, K. Black, C. Bernard, T. Childress, L. Dell'Asta, and N. Vignaroli. Prospects for Single
1502 Production of Vector-Like Quarks at 14 and 33 TeV. *Snowmass white paper, in preparation*, 2013.
- 1503 [177] E. Varnes. Potential of future accelerators for observing vector-like bottom-partner pair production.
1504 *Snowmass white paper, in preparation*, 2013.
- 1505 [178] Roberto Contino and Geraldine Servant. Discovering the top partners at the LHC using same-sign
1506 dilepton final states. *JHEP*, 0806:026, 2008, 0801.1679.
- 1507 [179] A. Avetisyan and T. Bose. Search for top partners with charge $5e/3$. *Snowmass white paper, in*
1508 *preparation*, 2013.
- 1509 [180] Robert M. Harris, Christopher T. Hill, and Stephen J. Parke. Cross-section for topcolor Z-prime(t)
1510 decaying to t anti-t: Version 2.6. 1999, hep-ph/9911288.
- 1511 [181] ATLAS Collaboration. A search for ttbar resonances in the lepton plus jets final state with ATLAS
1512 using 4.7 fb^{-1} of pp collisions at $\sqrt{s} = 7$ TeV. 2013, 1305.2756.
- 1513 [182] CMS Collaboration. Search for $t\bar{t}$ resonances in semileptonic final states in pp collisions at $\sqrt{s} = 8$
1514 TeV. *CMS-PAS-B2G-12-006*, 2013.
- 1515 [183] ATLAS Collaboration. Search for resonances decaying into top-quark pairs using fully hadronic decays
1516 in pp collisions with ATLAS at $\sqrt{s} = 7$ TeV. *JHEP*, 1301:116, 2013, 1211.2202.
- 1517 [184] CMS Collaboration. Search for anomalous top quark pair production in the boosted all-hadronic final
1518 state using pp collisions at $\sqrt{s} = 8$ TeV. *CMS-PAS-B2G-12-005*, 2013.

- 1519 [185] Kaustubh Agashe, Alexander Belyaev, Tadas Krupovnickas, Gilad Perez, and Joseph Virzi. LHC
1520 Signals from Warped Extra Dimensions. *Phys.Rev.*, D77:015003, 2008, hep-ph/0612015.
- 1521 [186] Vernon Barger, Tao Han, and Devin G.E. Walker. Top Quark Pairs at High Invariant Mass: A
1522 Model-Independent Discriminator of New Physics at the LHC. *Phys.Rev.Lett.*, 100:031801, 2008, hep-
1523 ph/0612016.
- 1524 [187] I. Iashvili, S. Jain, A. Kharchilava, and H. B. Prosper. Searching for $t\bar{t}$ resonances in dilepton+jets
1525 final states. *Snowmass white paper, in preparation*, 2013.
- 1526 [188] Leandro G. Almeida, Seung J. Lee, Gilad Perez, George Sterman, and Ilmo Sung. Template Overlap
1527 Method for Massive Jets. *Phys.Rev.*, D82:054034, 2010, 1006.2035.
- 1528 [189] Mihailo Backovic, Jose Juknevič, and Gilad Perez. Boosting the Standard Model Higgs Signal with
1529 the Template Overlap Method. 2012, 1212.2977.
- 1530 [190] M. Backovic and S. J. Lee. Searches for RS KK -gluons with the Template Overlap Method in the
1531 high end of boosted top regime. *Snowmass white paper, in preparation*, 2013.
- 1532 [191] ATLAS Collaboration. Search for $t\bar{b}$ resonances in proton-proton collisions at $\sqrt{s} = 7$ TeV with the
1533 ATLAS detector. *Phys.Rev.Lett.*, 109:081801, 2012, 1205.1016.
- 1534 [192] ATLAS Collaboration. Search for $w' \rightarrow t\bar{b}$ in proton-proton collisions at a centre-of-mass energy of
1535 $\sqrt{s} = 8$ tev with the atlas detector. Technical Report ATLAS-CONF-2013-050, CERN, Geneva, May
1536 2013.
- 1537 [193] CMS Collaboration. Search for a W' boson decaying to a bottom quark and a top quark in pp collisions
1538 at $\sqrt{s} = 7$ TeV. *Phys.Lett.*, B718:1229–1251, 2013, 1208.0956.
- 1539 [194] E. Drueke, B. Schoenrock, B. Alvarez Gonzalez, and R. Schwienhorst. Searches for resonances in the
1540 $t\bar{b}$ and $t\bar{c}$ final states at the high-luminosity LHC. 2013.
- 1541 [195] Priscila M. Aquino, Gustavo Burdman, and Oscar J.P. Eboli. A Signal for a theory of flavor at the
1542 LHC. *Phys.Rev.Lett.*, 98:131601, 2007, hep-ph/0612055.
- 1543 [196] M. Artuso, M. Papucci, and S. Prell. Flavor Mixing and CP Violation at High Energy. *Snowmass*
1544 *whitepaper, in preparation*, 2013.
- 1545 [197] Joseph Nutter, Reinhard Schwienhorst, Devin G.E. Walker, and Jiang-Hao Yu. Single Top Production
1546 as a Probe of B-prime Quarks. *Phys.Rev.*, D86:094006, 2012, 1207.5179.
- 1547 [198] ATLAS Collaboration. Search for single b^* -quark production with the ATLAS detector at $\sqrt{s} = 7$
1548 TeV. *Phys.Lett.*, B721:171–189, 2013, 1301.1583.
- 1549 [199] R. Calkins, Chekanov S., Dolen J., Pilot J., Pöschl R., and Tweedie. B. Reconstructing top quarks
1550 at the upgraded LHC and at future accelerators. Summary of “Top algorithms and detectors” High
1551 Energy Frontier Study Group. 2013.
- 1552 [200] S. Oryn, X. Rouby, and V. Lemaitre. DELPHES, a framework for fast simulation of a generic collider
1553 experiment. 2009, 0903.2225.
- 1554 [201] Matteo Cacciari, Gavin P. Salam, and Gregory Soyez. The anti- k_t jet clustering algorithm. *JHEP*,
1555 04:063, 2008, 0802.1189.
- 1556 [202] ATLAS Collaboration. Measurement of the top quark mass from 2011 atlas data using the template
1557 method. Technical Report ATLAS-CONF-2011-120, CERN, Geneva, Aug 2011.

- 1558 [203] A. Abdesselam, E. Bergeaas Kuutmann, U. Bitenc, G. Brooijmans, J. Butterworth, et al. Boosted
1559 objects: A Probe of beyond the Standard Model physics. *Eur.Phys.J.*, C71:1661, 2011, 1012.5412.
- 1560 [204] A. Altheimer, S. Arora, L. Asquith, G. Brooijmans, J. Butterworth, et al. Jet Substructure at the
1561 Tevatron and LHC: New results, new tools, new benchmarks. *J.Phys.*, G39:063001, 2012, 1201.0008.
- 1562 [205] Stephen D. Ellis, Christopher K. Vermilion, and Jonathan R. Walsh. Recombination Algorithms and
1563 Jet Substructure: Pruning as a Tool for Heavy Particle Searches. 2009, 0912.0033.
- 1564 [206] Stephen D. Ellis, Christopher K. Vermilion, and Jonathan R. Walsh. Techniques for improved heavy
1565 particle searches with jet substructure. *Phys. Rev.*, D 80:051501, 2009, 0903.5081.
- 1566 [207] David Krohn, Jesse Thaler, and Lian-Tao Wang. Jet Trimming. *JHEP*, 1002:084, 2010, 0912.1342.
- 1567 [208] Jonathan M. Butterworth, Adam R. Davison, Mathieu Rubin, and Gavin P. Salam. Jet substructure
1568 as a new higgs search channel at the lhc. *Phys. Rev. Lett.*, 100:242001, 2008.
- 1569 [209] Ben Lillie, Lisa Randall, and Lian-Tao Wang. The Bulk RS KK-gluon at the LHC. *JHEP*, 09:074,
1570 2007, hep-ph/0701166.
- 1571 [210] J. M. Butterworth, John R. Ellis, and A. R. Raklev. Reconstructing sparticle mass spectra using
1572 hadronic decays. *JHEP*, 05:033, 2007, hep-ph/0702150.
- 1573 [211] Leandro G. Almeida, Seung J. Lee, Gilad Perez, Ilmo Sung, and Joseph Virzi. Top Jets at the LHC.
1574 *Phys. Rev.*, D 79:074012, 2009, 0810.0934.
- 1575 [212] Leandro G. Almeida et al. Substructure of high- p_T Jets at the LHC. *Phys. Rev.*, D 79:074017, 2009,
1576 0807.0234.
- 1577 [213] David E. Kaplan, Keith Rehermann, Matthew D. Schwartz, and Brock Tweedie. Top Tagging: A
1578 Method for Identifying Boosted Hadronically Decaying Top Quarks. *Phys. Rev. Lett.*, 101:142001,
1579 2008, 0806.0848.
- 1580 [214] Gustaaf H Brooijmans. High p_T Hadronic Top Quark Identification. Published in "A Les Houches
1581 Report. Physics at Tev Colliders 2007 – New Physics Working Group", 2008, hep-ph/0802.3715.
- 1582 [215] Jonathan M. Butterworth et al. Discovering baryon-number violating neutralino decays at the LHC.
1583 Technical Report CERN-PH-TH/2009-073, hep-ph/0906.0728, 2009.
- 1584 [216] ATLAS Collaboration. Reconstruction of high mass $t\bar{t}$ resonances in the lepton+jets channel. Technical
1585 Report ATL-PHYS-PUB-2009-081. ATL-COM-PHYS-2009-255, CERN, Geneva, May 2009.
- 1586 [217] CMS Collaboration. A cambridge-aachen (c-a) based jet algorithm for boosted top-jet tagging.
1587 Technical Report CMS-PAS-JME-09-001, CERN, Jul 2009.
- 1588 [218] Christoph Hackstein and Michael Spannowsky. Boosting Higgs discovery - the forgotten channel, 2010,
1589 hep-ph:1008.2202, 1008.2202.
- 1590 [219] S. Chekanov and J. Proudfoot. Searches for TeV-scale particles at the LHC using jet shapes. *Phys.*
1591 *Rev.*, D81:114038, 2010.
- 1592 [220] S. V. Chekanov, C. Levy, J. Proudfoot, and R. Yoshida. New approach for jet-shape identification of
1593 TeV-scale particles at the LHC. *Phys. Rev.*, D82:094029, 2010.
- 1594 [221] ATLAS Collaboration. Prospects for top anti-top resonance searches using early atlas data. Technical
1595 Report ATL-PHYS-PUB-2010-008, CERN, Geneva, Jul 2010.

- 1596 [222] Jesse Thaler and Ken Tilburg. Identifying boosted objects with n-subjettiness. *Journal of High Energy*
1597 *Physics*, 2011(3):1–28, 2011.
- 1598 [223] ATLAS Collaboration. Performance of jet substructure techniques for large-R jets in proton-proton
1599 collisions at $\sqrt{s} = 7$ TeV using the ATLAS detector. 2013, 1306.4945.
- 1600 [224] ATLAS Collaboration. Jet mass and substructure of inclusive jets in $\sqrt{s} = 7$ TeV *pp* collisions with
1601 the ATLAS experiment. *JHEP*, 1205:128, 2012, 1203.4606.
- 1602 [225] ATLAS Collaboration. A search for $t\bar{t}$ resonances in lepton+jets events with highly boosted top quarks
1603 collected in *pp* collisions at $\sqrt{s} = 7$ TeV with the ATLAS detector. *JHEP*, 1209:041, 2012, 1207.2409.
- 1604 [226] M.J. Oreglia. A Study of the Reactions ψ prime to $\gamma \gamma \psi$,. Ph.D. Thesis, SLAC-R-236,
1605 1980.
- 1606 [227] S. Catani, Yuri L. Dokshitzer, M. H. Seymour, and B. R. Webber. Longitudinally invariant K_t
1607 clustering algorithms for hadron hadron collisions. *Nucl. Phys.*, B406:187–224, 1993.
- 1608 [228] Stephen D. Ellis and Davison E. Soper. Successive combination jet algorithm for hadron collisions.
1609 *Phys. Rev.*, D48:3160–3166, 1993, hep-ph/9305266.
- 1610 [229] ATLAS Collaboration. Jet energy resolution in proton-proton collisions at $\sqrt{s} = 7$ TeV recorded in
1611 2010 with the ATLAS detector. *Eur.Phys.J.*, C73:2306, 2013, 1210.6210.